Heteronuclear Decoupling and Recoupling

Christopher Jaroniec, Ohio State University

1. Brief review of nuclear spin interactions, MAS, etc.
2. Heteronuclear decoupling (average Hamiltonian analysis of CW decoupling, intro to improved decoupling schemes)
3. Heteronuclear recoupling (R^3, REDOR)
4. AHT analysis of finite pulse REDOR
5. ^{13}C-^{15}N distance measurements in multispin systems (frequency selective REDOR, 3D TEDOR methods)
6. Intro to dipole tensor correlation experiments for measuring torsion angles

Isolated Spin-1/2 (I-S) System

$$H_{int} = H_I^{CS} + H_S^{CS} + H_{IS}^{J} + H_{IS}^{D}$$

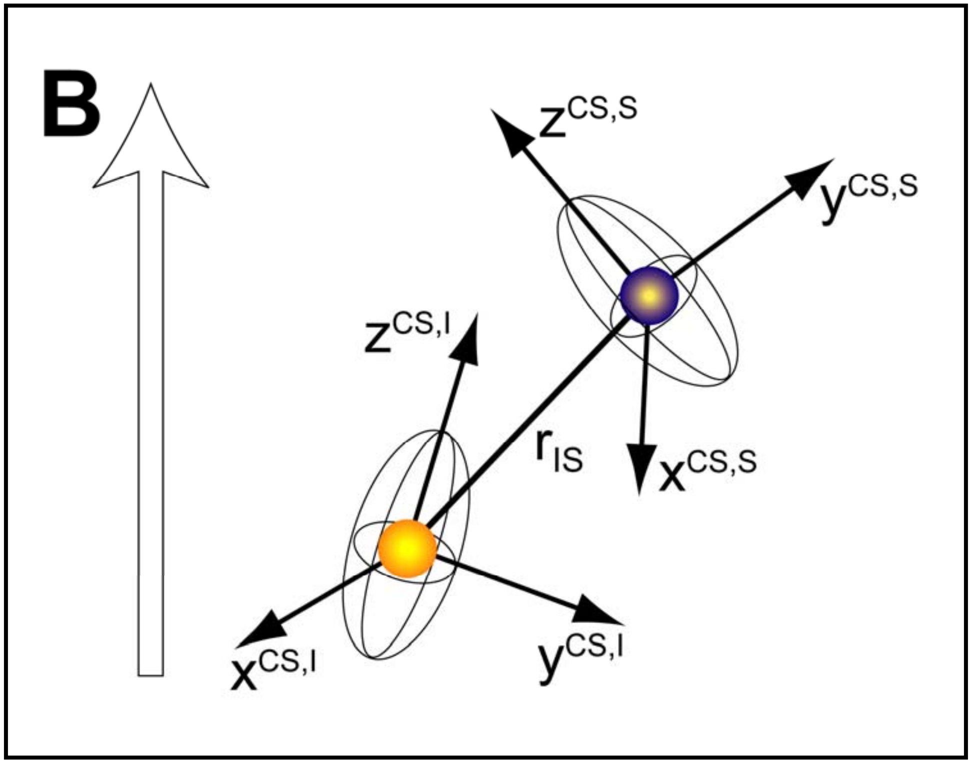

$$H_I^{CS} = \gamma_I \mathbf{I} \cdot \boldsymbol{\sigma} \cdot \mathbf{B}$$

$$H_{IS}^{D} = \mathbf{I} \cdot \mathbf{D}_{IS} \cdot \mathbf{S}$$

$$H_{IS}^{J} = 2\pi \mathbf{I} \cdot \mathbf{J}_{IS} \cdot \mathbf{S}$$

- Relevant interactions expressed in general as coupling of two vectors by a 2nd rank Cartesian tensor (3 x 3 matrix)

Rotate Tensors: PAS → Lab

$$\boldsymbol{\sigma}_{LAB} = \mathbf{R}(\Omega) \cdot \boldsymbol{\sigma}_{PAS} \cdot \mathbf{R}(\Omega)^{-1}; \quad \Omega = \{\alpha, \beta, \gamma\}$$

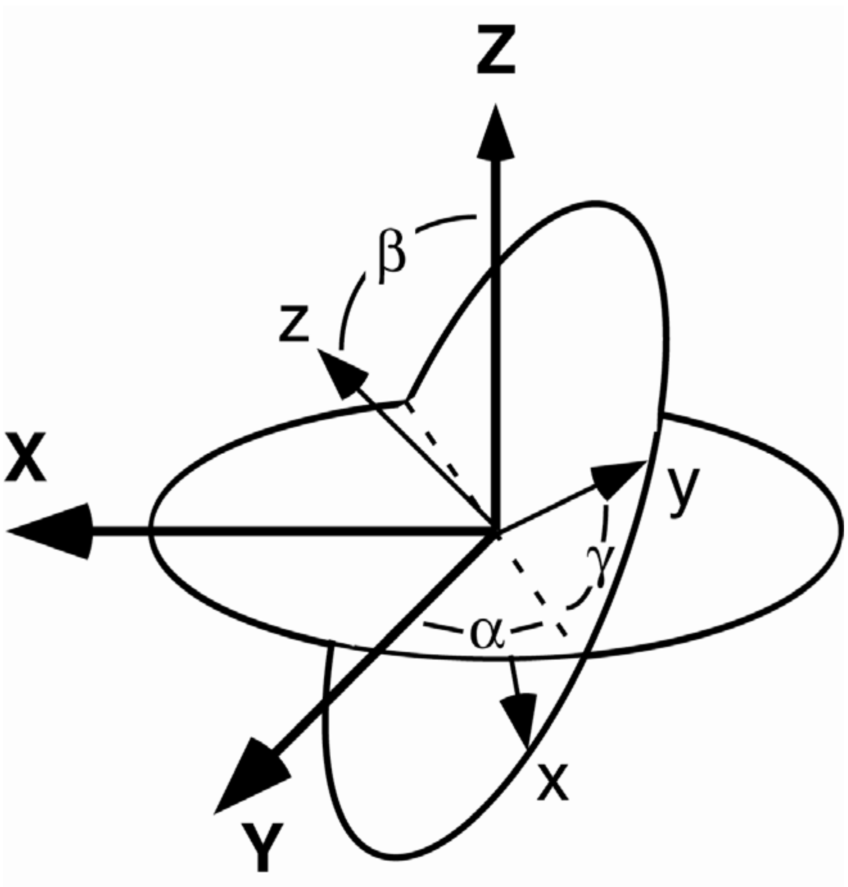

- SSNMR spectra determined by interactions in lab frame
- Rotate tensors from their principal axis systems (matrices diagonal) into lab frame (B_0 || z-axis)
- In general, a rotation is accomplished using a set of 3 Euler angles $\{\alpha,\beta,\gamma\}$

Multiple Interactions

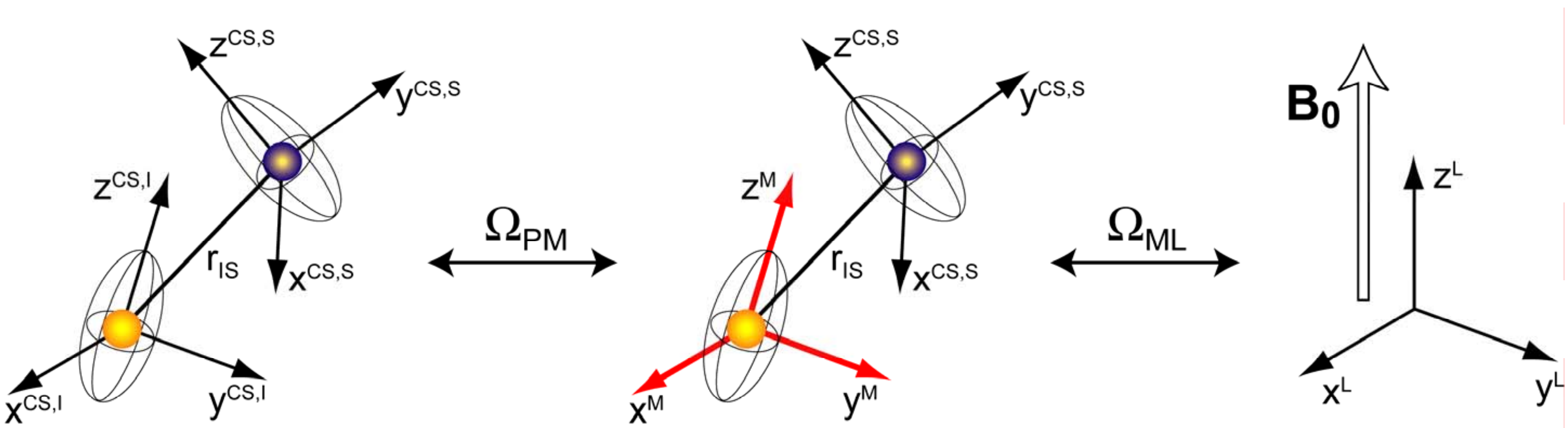

- In case of multiple interactions first transform all tensors into common frame (molecular- or crystallite-fixed frame)
- Powder samples: rotate each crystallite into lab frame

High Field Truncation: H_{CS}

$$H_I^{CS} = \gamma_I B_0 \sigma_{zz}^{LAB} I_z = \gamma_I B_0 \left(\sigma_{xx} \sin^2\theta \cos^2\phi + \sigma_{yy} \sin^2\theta \sin^2\phi + \sigma_{zz} \cos^2\theta \right) I_z$$

$$= \left\{ \gamma_I B_0 \sigma_{iso} + \gamma_I B_0 \delta \frac{1}{2} \left[3\cos^2\theta - 1 - \eta \sin^2\theta \cos(2\phi) \right] \right\} I_z$$

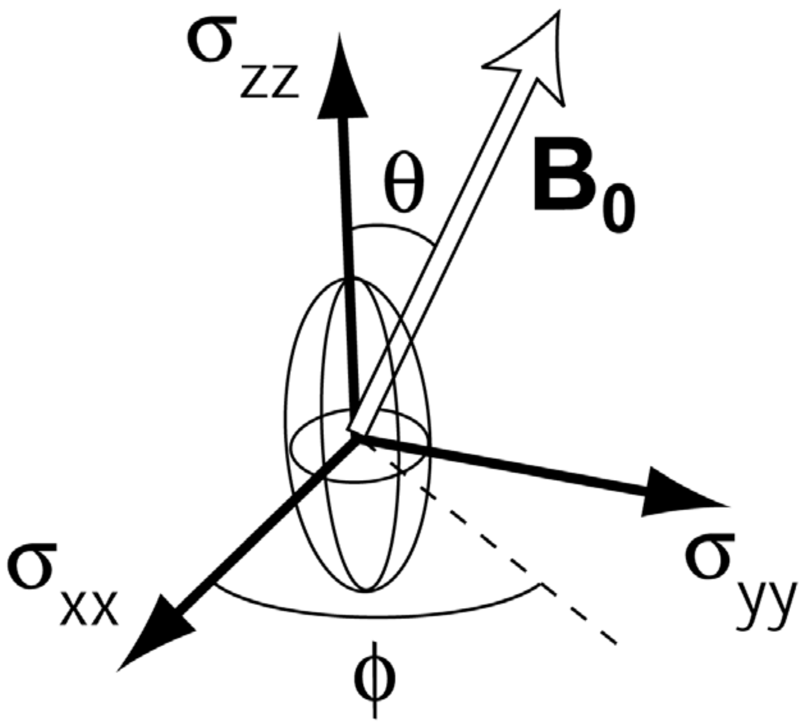

$$\sigma_{iso} = \frac{1}{3}\left(\sigma_{xx} + \sigma_{yy} + \sigma_{zz} \right)$$

$$\delta = \sigma_{zz} - \sigma_{iso}$$

$$\eta = \frac{\sigma_{yy} - \sigma_{xx}}{\delta}$$

• Retain only parts of H^{CS} that commute with I_z

High Field Truncation: H_J and H_D

$$H_{IS}^{J} = \pi J_{IS} 2 I_z S_z$$

$$H_{IS}^{D} = b_{IS} \frac{1}{2}\left(3\cos^2\theta - 1\right) 2 I_z S_z$$

$$b_{IS} = -\frac{\mu_0}{4\pi}\frac{\gamma_I \gamma_S}{r_{IS}^3}$$

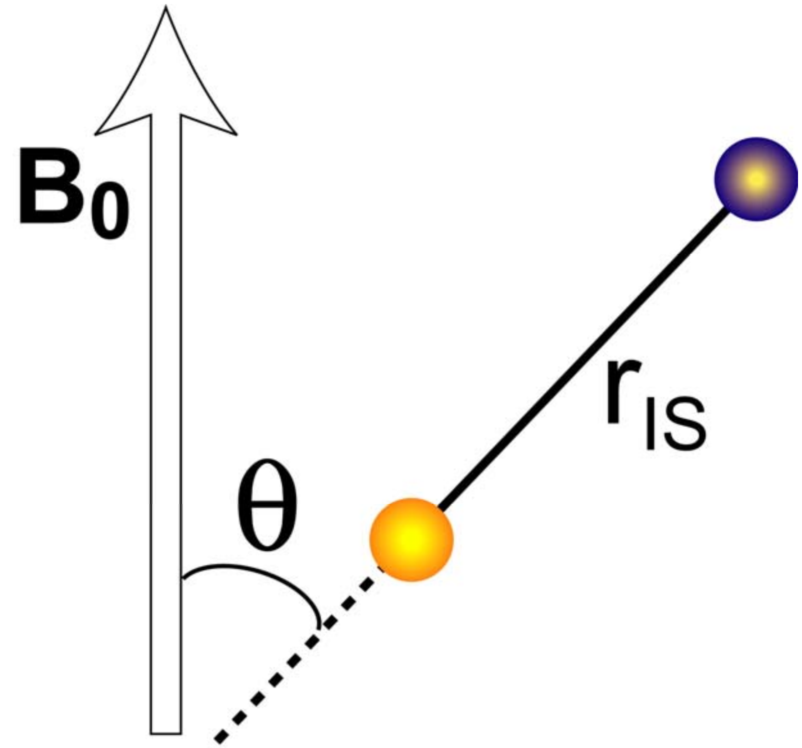

- J-anisotropy negligible in most cases
- b_{IS} in rad/s; directly related to I-S distance

Dipolar Couplings in Proteins

Spin 1	Spin 2	r_{12} (Å)	$b_{12}/2\pi$ (Hz)
^{1}H	^{13}C	1.12	~21,500
^{1}H	^{15}N	1.04	~10,800
^{13}C	^{13}C	1.5	~2,200
^{13}C	^{15}N	1.5	~900
^{13}C	^{15}N	2.5	~200
^{13}C	^{15}N	4.0	~50

Static Powder Spectra: H_{CS} & H_D

$$\langle I^+(t)\rangle \propto \int d\phi \int d\theta \sin\theta \cdot \mathrm{Tr}\left\{I^+ \exp\left(-iH_{CS}t\right) I_x \exp\left(iH_{CS}t\right)\right\}$$

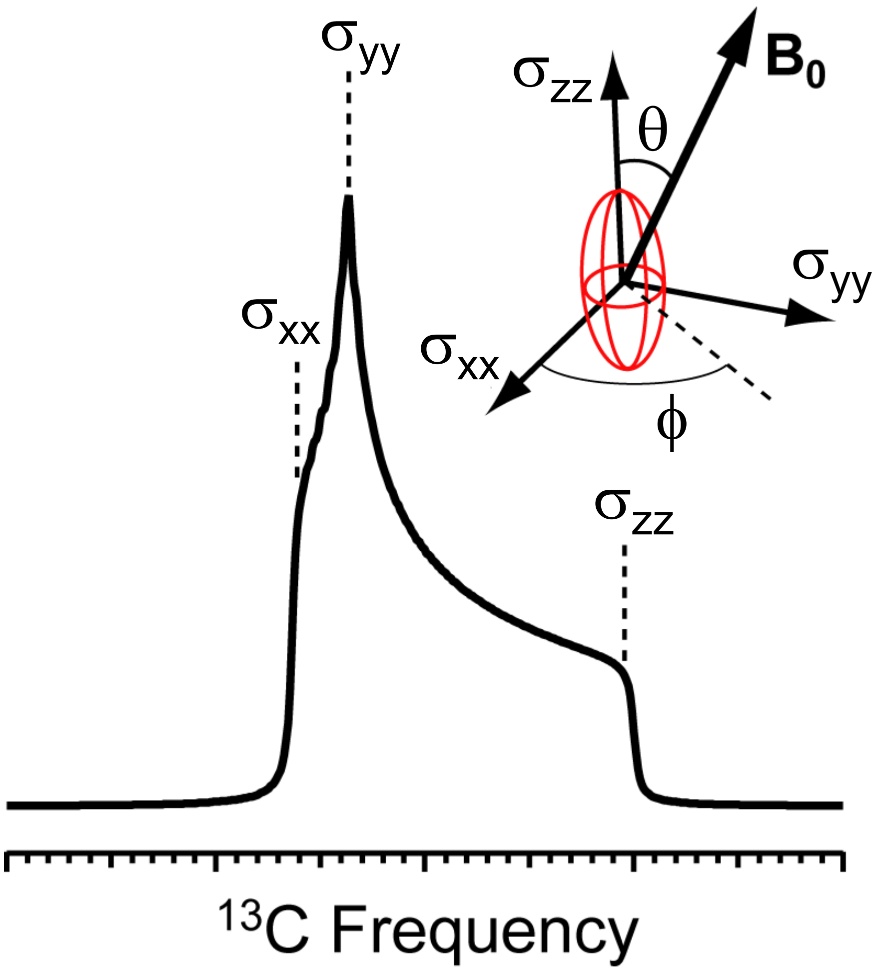

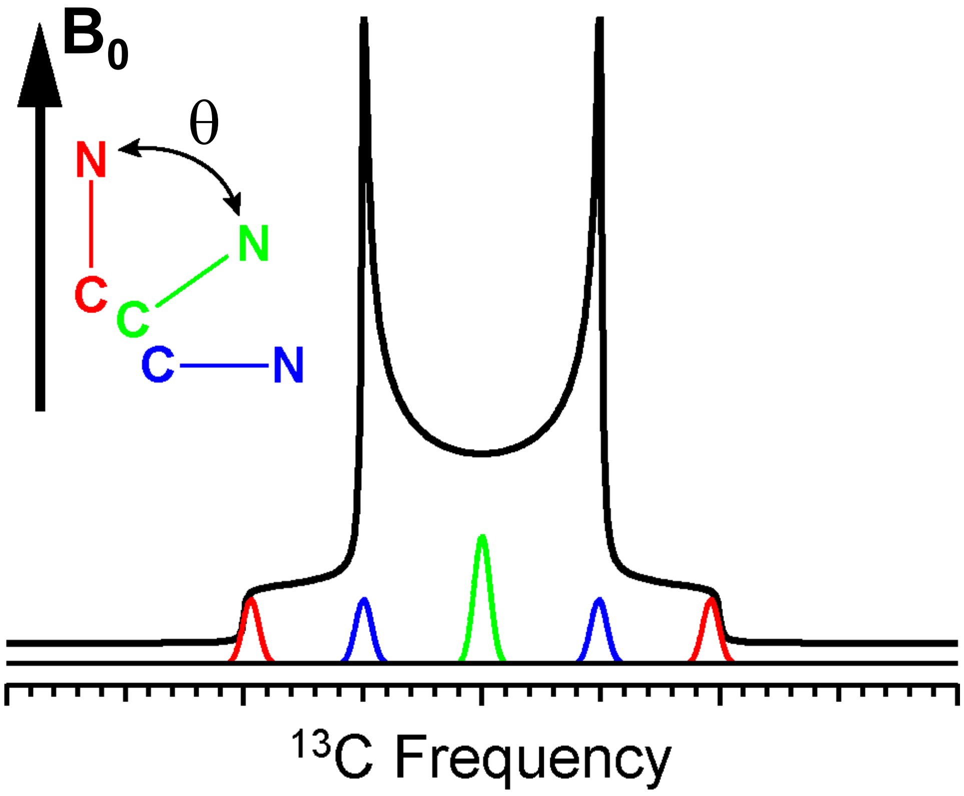

NMR of Rotating Samples

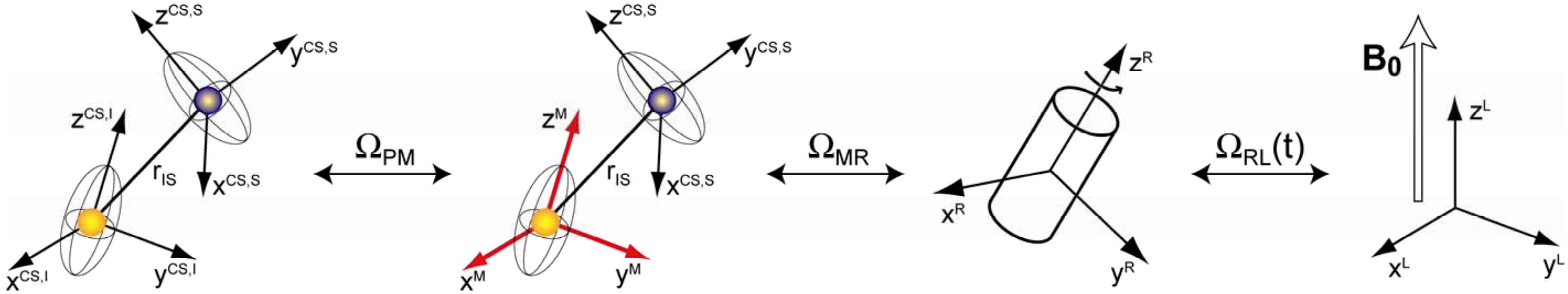

$$H_I^{CS} = \omega_I(t) I_z$$

$$H_{IS}^{D} = \omega_{IS}(t) 2 I_z S_z$$

$$H_{IS}^{J} = \pi J_{IS} 2 I_z S_z$$

$$\omega_\lambda(t) = \sum_{m=-2}^{2} \omega_\lambda^{(m)} \exp\{ i m \omega_r t \}$$

H_D *for Rotation at Magic Angle* (θ_m = 54.74°)

$$H_{IS}^{D} = \left\{ \sum_{m=-2}^{2} \omega_{IS}^{(m)} \exp\left(im\omega_r t \right) \right\} 2I_z S_z$$

$$\omega_{IS}^{(0)} = b_{IS} \frac{\left(3\cos^2 \beta_{PR} - 1\right)}{2} \frac{\left(3\cos^2 \theta_m - 1\right)}{2} = 0$$

$$\omega_{IS}^{(\pm 1)} = -\frac{b_{IS}}{2\sqrt{2}} \sin\left(2\beta_{PR}\right) \exp\left\{\pm i\gamma_{PR}\right\}$$

$$\omega_{IS}^{(\pm 2)} = \frac{b_{IS}}{4} \sin^2 \beta_{PR} \exp\left\{\pm i2\gamma_{PR}\right\}$$

- For spinning at the magic angle the time-independent dipolar (and CSA) components vanish; terms modulated at ω_r and $2\omega_r$ vanish when averaged over the rotor cycle

^{13}C-^{1}H Dipolar Spectra under MAS

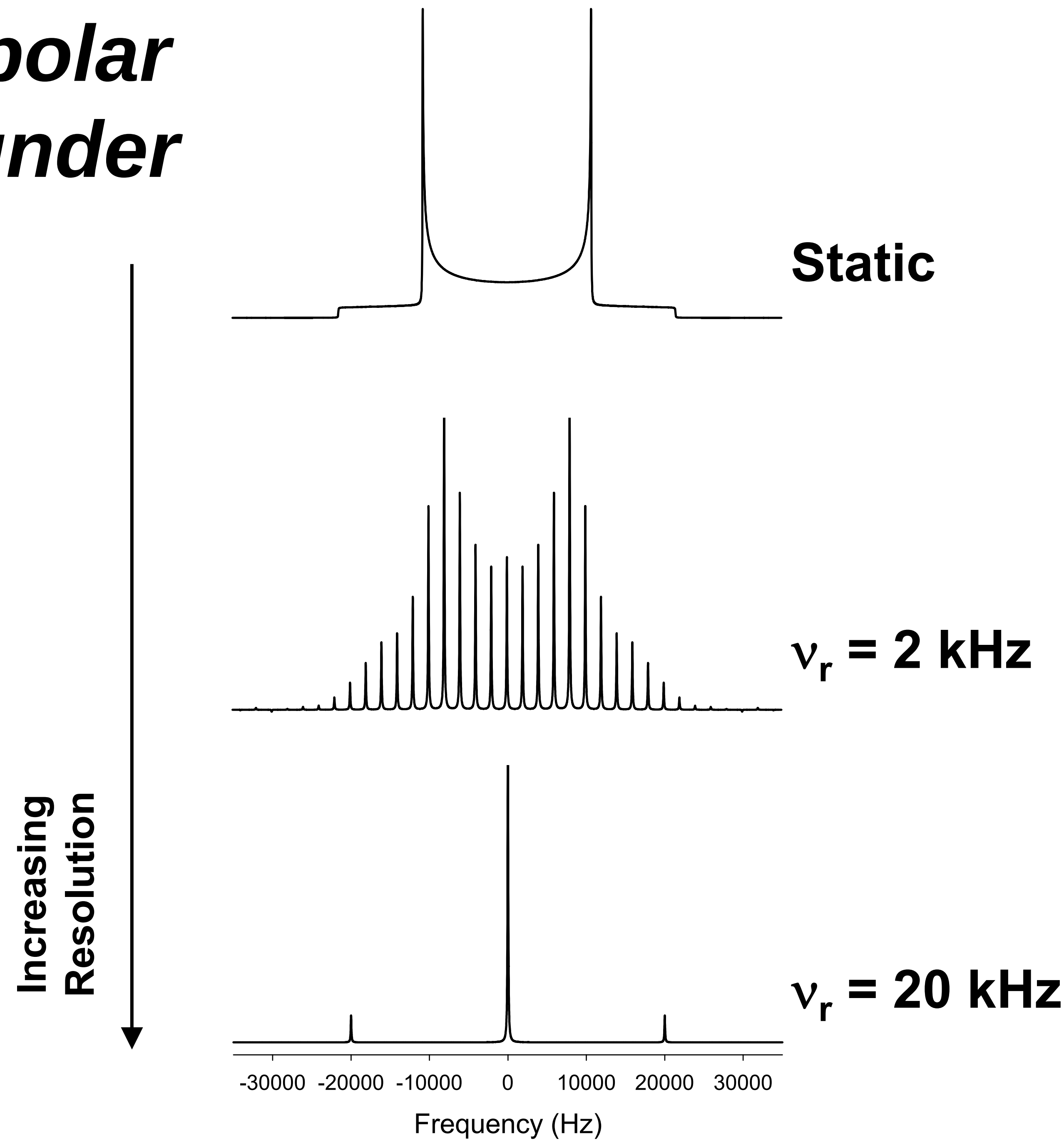

^{13}C SSNMR Spectra at High MAS Rates

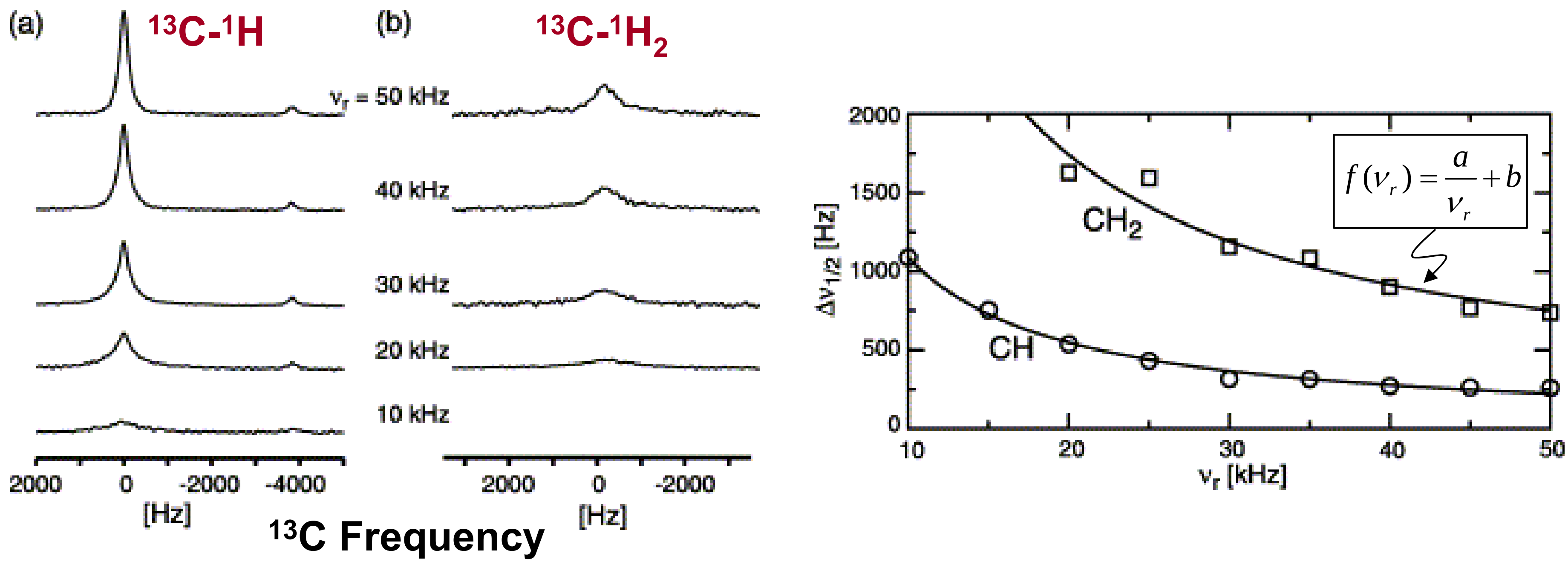

- Presence of many strong ^{1}H-^{1}H couplings leads to an incomplete averaging of ^{13}C-^{1}H dipolar coupling by MAS

M. Ernst, JMR 2003

High-Power CW Decoupling

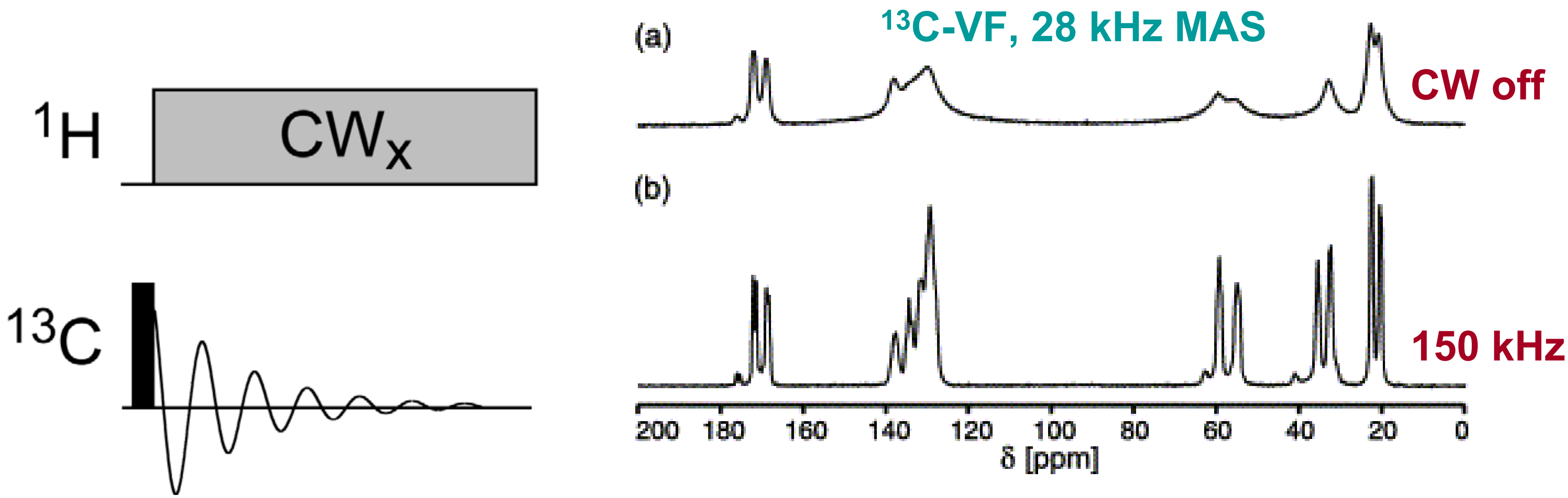

- Average ^{13}C-^{1}H couplings by simultaneously using MAS and high-power ^{1}H RF irradiation
- Traditionally for efficient decoupling ^{1}H RF fields of ~50-200 kHz were used (i.e., $\omega_{1H} >> b_{HH}, b_{HX}$)

CW Decoupling: AHT Analysis

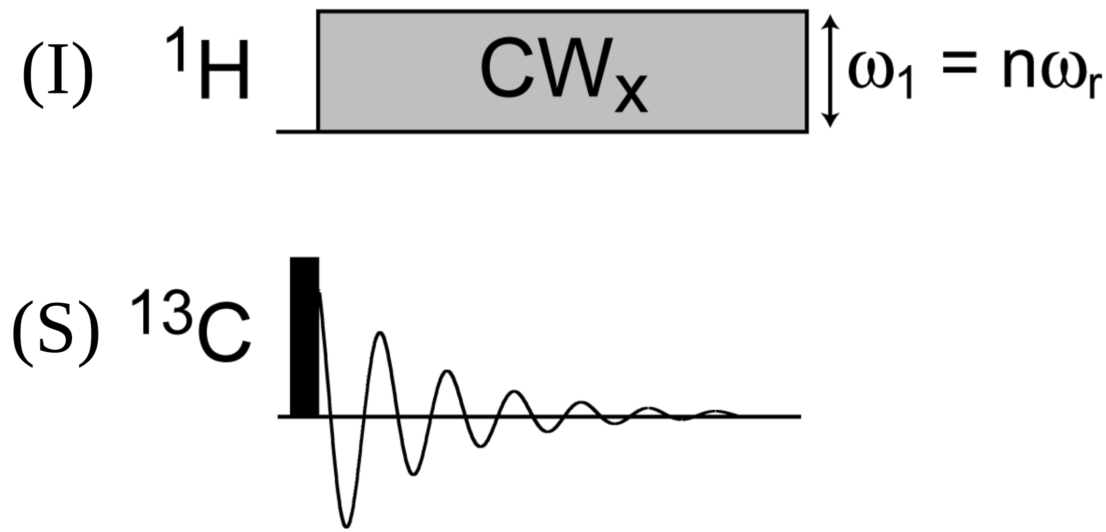

$$H_{tot} = \omega_S^{iso} S_z + \omega_S(t) S_z + \omega_I^{iso} I_z + \omega_I(t) I_z$$
$$+\pi J_{IS} 2I_z S_z + \omega_{IS}(t) 2I_z S_z + \omega_1 I_x$$

- Average Hamiltonian analysis: RF and MAS modulations must be synchronized to obtain cyclic propagator

AHT: Summary

$$\rho(t) = U_{tot}(t)\rho(0)U_{tot}(t)^{-1}; \quad U_{tot}(t) = T\exp\left\{-i\int_0^t dt'(H + H_{RF})\right\}$$

$$U_{tot}(t) = U_{RF}(t)U(t) = U_{RF}(t)\cdot T\exp\left\{-i\int_0^t dt'\tilde{H}\right\}; \quad \tilde{H} = U_{RF}^{-1}HU_{RF}$$

$$U_{tot}(t_c) = U(t_c) = T\exp\left\{-i\int_0^{t_c} dt'\tilde{H}\right\} = \exp\left\{-i\bar{\tilde{H}}t_c\right\} \quad (\text{for } U_{RF}(t_c) = 1)$$

$$\bar{\tilde{H}} = \bar{\tilde{H}}^{(0)} + \bar{\tilde{H}}^{(1)} + \bar{\tilde{H}}^{(2)} + \ldots$$

$$\bar{\tilde{H}}^{(0)} = \frac{1}{t_c}\int_0^{t_c} dt'\tilde{H}; \quad \bar{\tilde{H}}^{(1)} = \frac{1}{2it_c}\int_0^{t_c} dt''\int_0^{t''} dt'\left[\tilde{H}(t''),\tilde{H}(t')\right]; \quad \ldots$$

Haeberlen & Waugh, Phys. Rev. 1968

Interaction Frame Hamiltonian

$$\tilde{H} = U_{RF}^{-1} H U_{RF} = \exp\left\{ i\omega_1 t I_x \right\} H \exp\left\{ -i\omega_1 t I_x \right\}$$

$$\tilde{H} = \tilde{H}_S + \tilde{H}_I + \tilde{H}_{IS}^J + \tilde{H}_{IS}^D$$

$$\tilde{H}_S = \omega_S^{iso} S_z + \omega_S(t) S_z$$

$$\tilde{H}_{IS}^J = \pi J_{IS} 2S_z \left\{ I_z \cos(\omega_1 t) + I_y \sin(\omega_1 t) \right\}$$

$$= \pi J_{IS} S_z \left\{ I_z \left(e^{in\omega_r t} + e^{-in\omega_r t} \right) - i I_y \left(e^{in\omega_r t} - e^{-in\omega_r t} \right) \right\}$$

$$\tilde{H}_{IS}^D = \omega_{IS}(t) 2S_z \left\{ I_z \cos(\omega_1 t) + I_y \sin(\omega_1 t) \right\}$$

$$= \omega_{IS}(t) S_z \left\{ I_z \left(e^{in\omega_r t} + e^{-in\omega_r t} \right) - i I_y \left(e^{in\omega_r t} - e^{-in\omega_r t} \right) \right\}$$

Interaction Frame Cont.

$$\tilde{H}_{IS}^{D} = \omega_{IS}(t) 2S_z \left\{ I_z \cos(\omega_1 t) + I_y \sin(\omega_1 t) \right\}$$

$$= \omega_{IS}(t) S_z \left\{ I_z \left(e^{in\omega_r t} + e^{-in\omega_r t} \right) - iI_y \left(e^{in\omega_r t} - e^{-in\omega_r t} \right) \right\}$$

$$= \sum_{m=-2}^{2} \{ \omega_{IS}^{(m)} \left[e^{i(m+n)\omega_r t} + e^{i(m-n)\omega_r t} \right] I_z S_z$$

$$-i\omega_{IS}^{(m)} \left[e^{i(m+n)\omega_r t} - e^{i(m-n)\omega_r t} \right] I_y S_z \}$$

Lowest-Order Average Hamiltonian

$$\bar{\tilde{H}}^{(0)} = \bar{\tilde{H}}_S^{(0)} + \bar{\tilde{H}}_{J,IS}^{(0)} + \bar{\tilde{H}}_{D,IS}^{(0)}$$

$$\bar{\tilde{H}}_S^{(0)} = \frac{\omega_S^{iso} S_z}{\tau_r} \int_0^{\tau_r} dt + \sum_{m=-2}^{2} \left\{ \frac{S_z}{\tau_r} \int_0^{\tau_r} dt \omega_S^{(m)} e^{im\omega_r t} \right\} = \omega_S^{iso} S_z$$

$$\bar{\tilde{H}}_{J,IS}^{(0)} = \frac{\pi J_{IS} S_z}{\tau_r} \int_0^{\tau_r} dt \left\{ I_z \left(e^{in\omega_r t} + e^{-in\omega_r t} \right) - iI_y \left(e^{in\omega_r t} - e^{-in\omega_r t} \right) \right\} = 0$$

- S-spin CSA refocused by MAS, I-S J-coupling eliminated by I-spin decoupling RF field

Lowest-Order Average H_D

$$\bar{\tilde{H}}_S^{(0)} = \frac{1}{\tau_r}\int_0^{\tau_r} dt \sum_{m=-2}^{2} \{\omega_{IS}^{(m)}\left[e^{i(m+n)\omega_r t} + e^{i(m-n)\omega_r t}\right] I_z S_z$$

$$- i\omega_{IS}^{(m)}\left[e^{i(m+n)\omega_r t} - e^{i(m-n)\omega_r t}\right] I_y S_z\}$$

$$\frac{1}{\tau_r}\int_0^{\tau_r} dt\omega_{IS}^{(m)} e^{i(m\pm n)\omega_r t} = \begin{cases} 0 & \text{if } m \pm n \neq 0 \\ \omega_{IS}^{(\mp n)} & \text{if } m \pm n = 0 \end{cases}$$

Lowest-Order Average H_D

$n \neq 1,2 \longrightarrow$ I-S Decoupling

$$\bar{\tilde{H}}^{(0)}_{D,IS} = 0$$

$n = 1,2 \longrightarrow$ I-S Dipolar Recoupling!

$$\bar{\tilde{H}}^{(0)}_{D,IS} = \left(\omega_{IS}^{(-n)} + \omega_{IS}^{(n)}\right) I_z S_z - i\left(\omega_{IS}^{(-n)} - \omega_{IS}^{(n)}\right) I_y S_z$$

- ***Rotary resonance recoupling*** (R^3) arises from the interference of MAS and I-spin RF (when $\omega_1 = \omega_r$ or $2\omega_r$)
- Additional (much-weaker) resonances (n = 3,4,…) are also possible due to higher order average Hamiltonian terms involving the I-spin CSA

Improved heteronuclear decoupling: Two pulse phase modulation (TPPM)

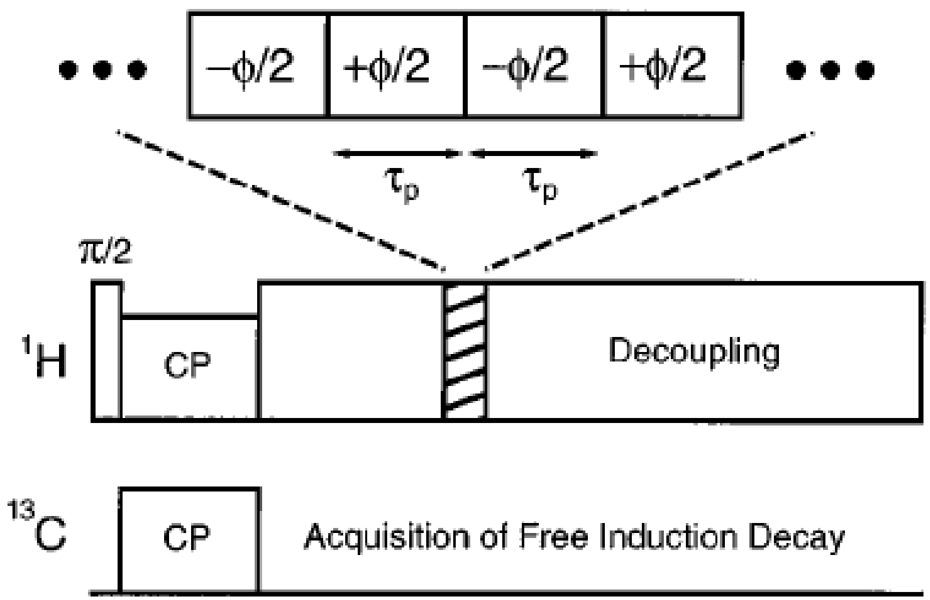

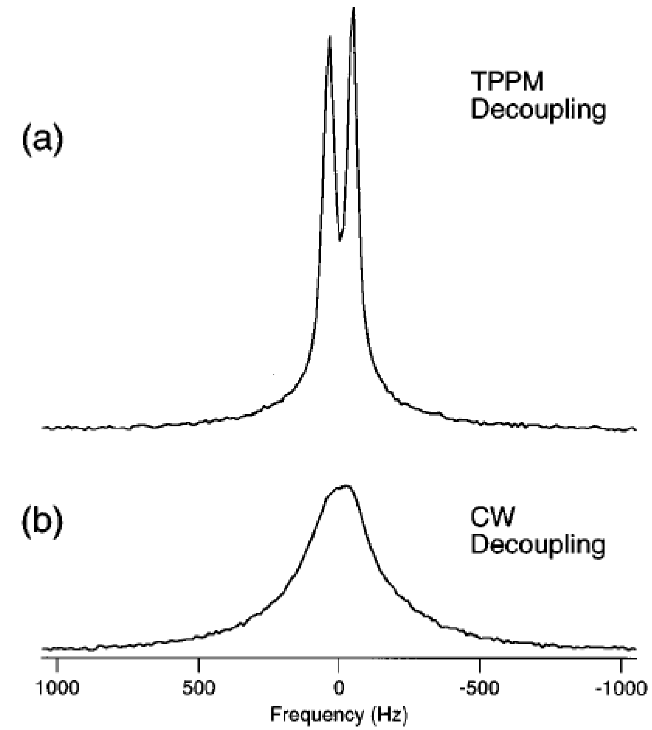

- The first truly effective pulse scheme (and still one of the best) for achieving efficient heteronuclear decoupling in samples under MAS
- TPPM reduces magnitude of cross-term between ^{1}H CSA and ^{1}H-X dipolar coupling which dominates the residual linewidth …

Bennett, Rienstra, Auger & Griffin, JCP 1995

Optimization of TPPM Decoupling

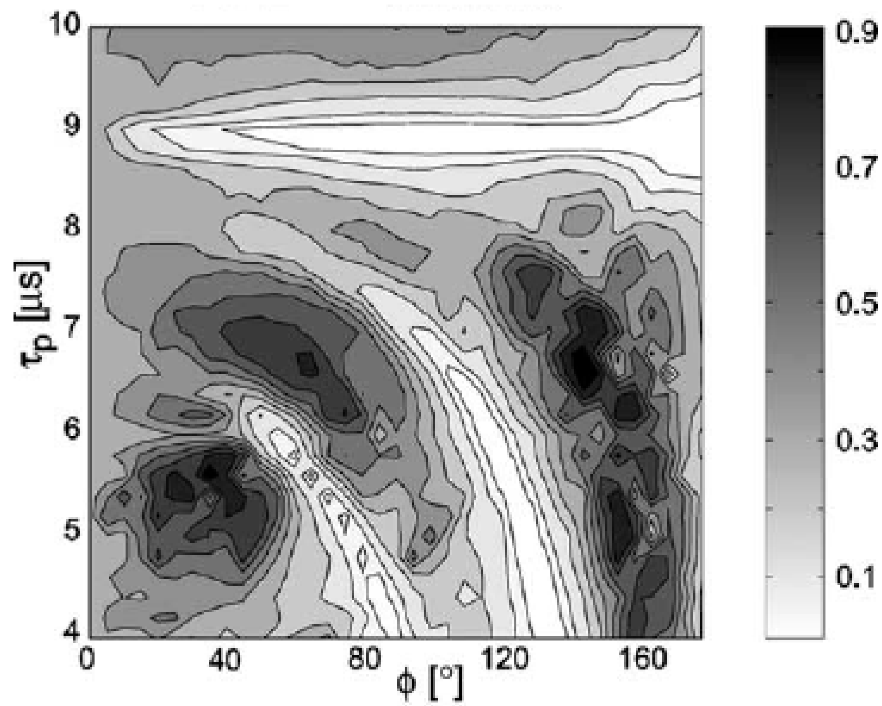

$$\phi \approx 10 - 50^{\circ}$$

$$\beta_p = \omega_{1,H} \tau_p \approx \pi$$

- Parameters optimized empirically
- Under moderate MAS rates (~10-25 kHz) and ^{1}H RF fields (~70-100 kHz) best results usually obtained for ϕ and β in ranges given above

Other Useful Decoupling Schemes

- TPPM-related schemes (similar to TPPM for most rigid solids):
  - FMPM (**Gan & Ernst, *SSNMR* 1997**) – frequency and phase modulated decoupling
  - SPINAL (**Fung et al., *JMR* 2000**) – TPPM combined with supercycles
- XiX (**Detken et al., *Chem. Phys. Lett.* 2002**) – offers improvements over TPPM at high MAS rates (>20 kHz) and high ^{1}H RF (>100 kHz)
- Low-power CW decoupling (~10 kHz) at very high MAS rates, 30-50+ kHz (**Ernst, Samoson & Meier, *Chem. Phys. Lett.* 2001**)

X inverse-X (XiX) Decoupling

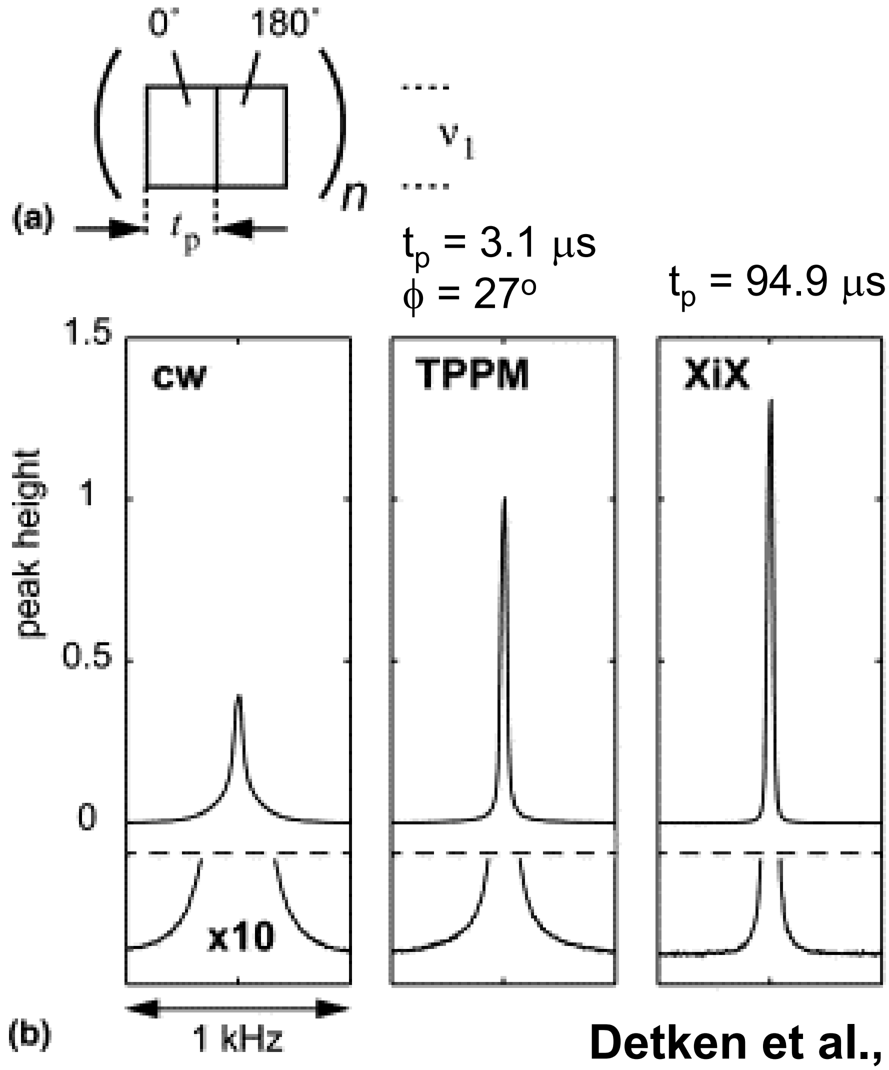

2-^{13}C alanine
ν_r = 30 kHz
ν_1 = 150 kHz

Detken et al., *Chem. Phys. Lett.* 2002

- Technically XiX is equivalent to TPPM with $\Delta\phi = 180^o$ but pulse width considerations are very different

XiX Decoupling

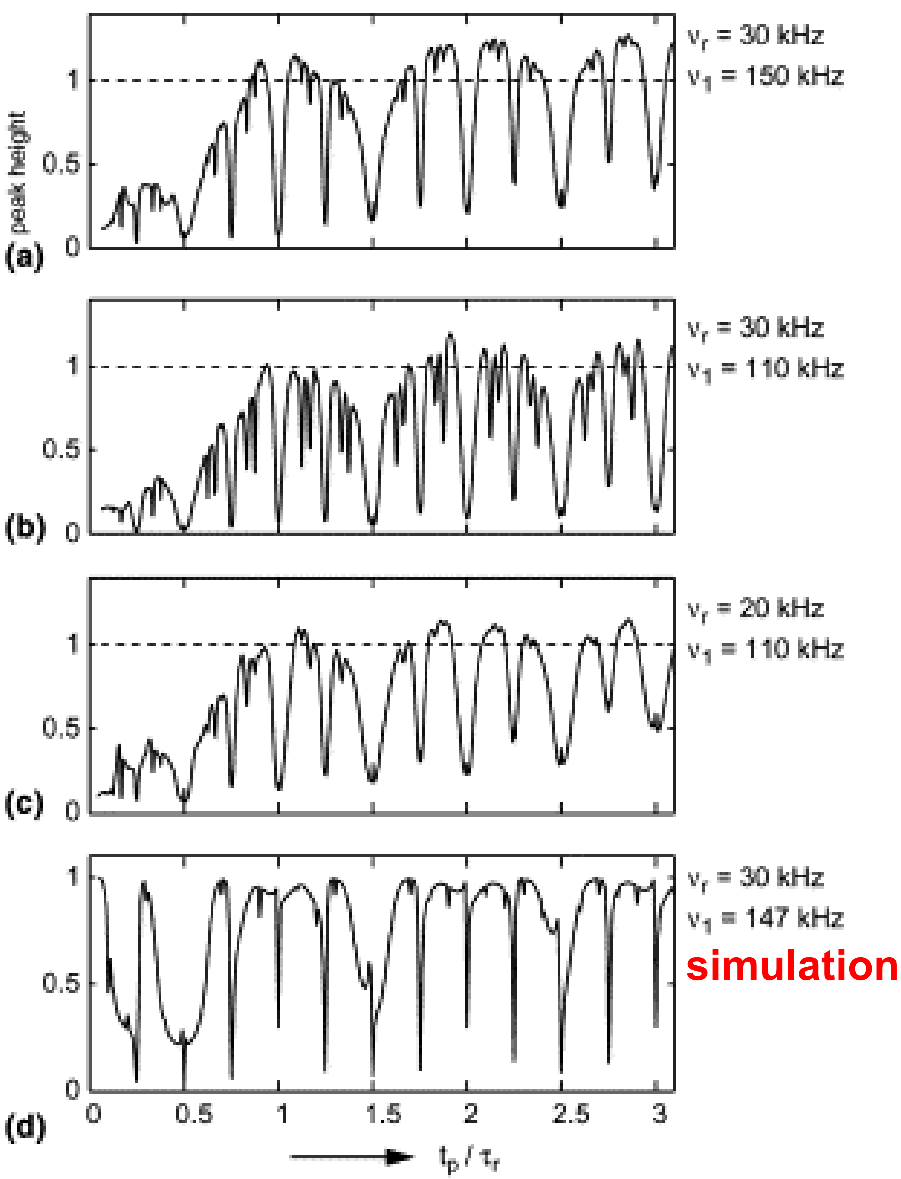

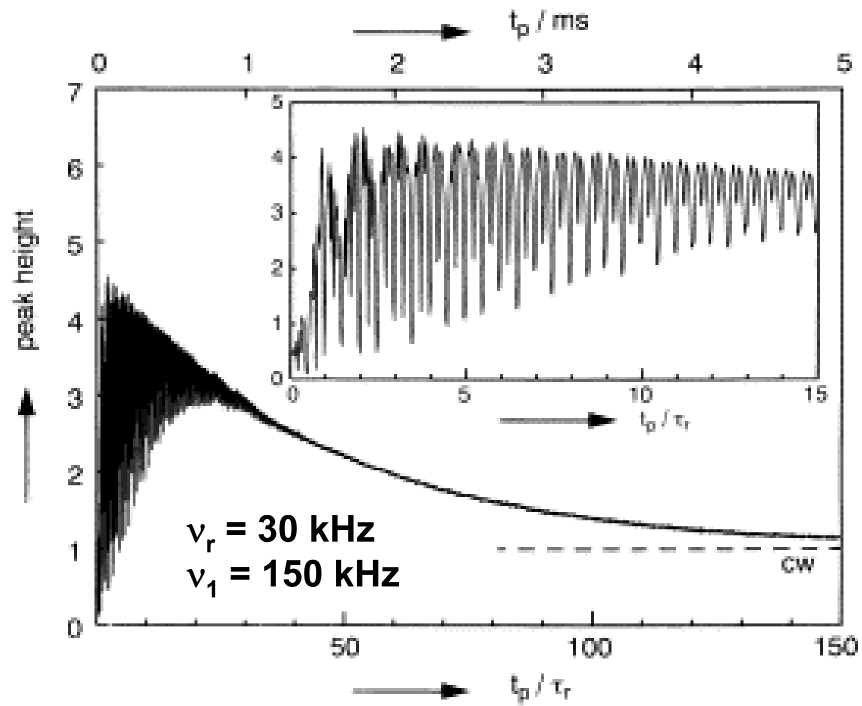

- Performance determined mainly by t_p in units of τ_r
- Best when $t_p > \tau_r$ (e.g., optimize around $2.85\tau_r$) and when strong resonances at $t_p = n\tau_r/4$ avoided

XiX Decoupling

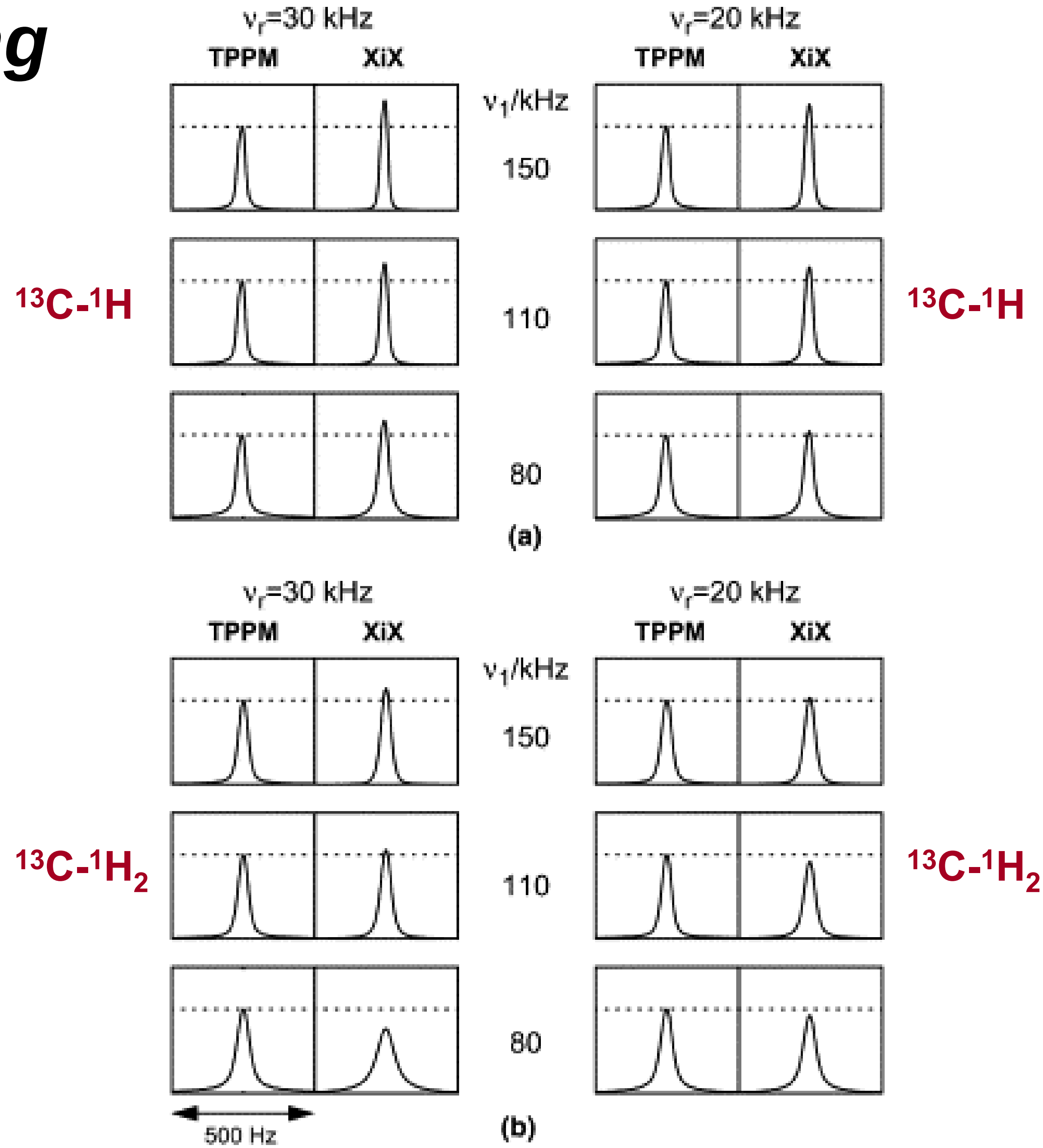

Rotary Resonance Recoupling

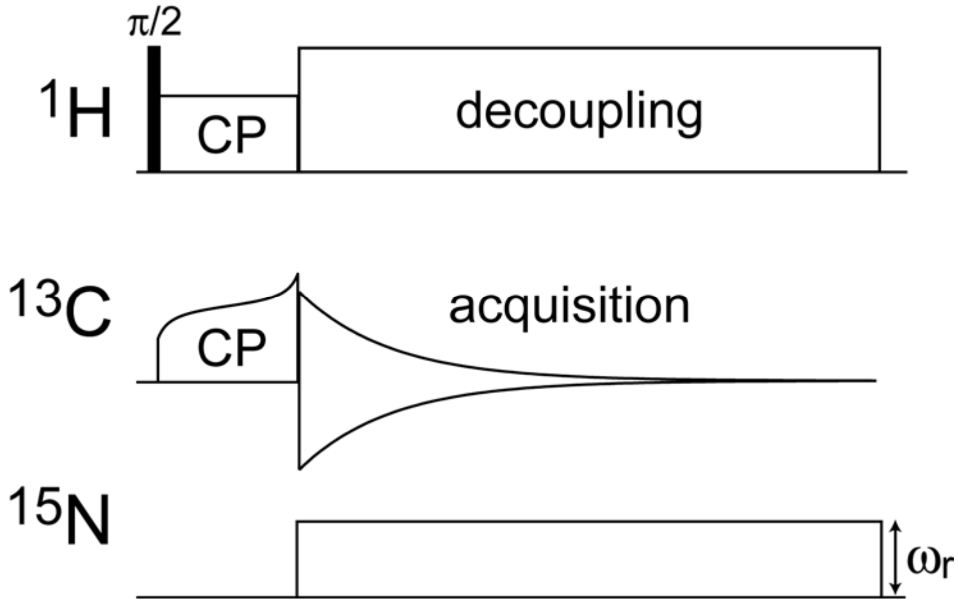

$$\bar{\tilde{H}}^{(0)}_{D,CN} = \left(\omega^{(-1)}_{IS} + \omega^{(1)}_{IS}\right) C_z N_z - i\left(\omega^{(-1)}_{IS} - \omega^{(1)}_{IS}\right) C_z N_y$$

$$= \exp\left\{-i\gamma_{PR} N_x\right\}\left(\tilde{\omega} 2 C_z N_z\right)\exp\left\{i\gamma_{PR} N_x\right\}$$

$$\tilde{\omega} = -\frac{1}{2\sqrt{2}} b_{IS} \sin(2\beta_{PR})$$

Oas, Levitt & Griffin, JCP 1988

Rotary Resonance Recoupling

$$\rho(t) = \exp\{-i\bar{\tilde{H}}^{(0)}_{D,CN} t\} C_x \exp\{i\bar{\tilde{H}}^{(0)}_{D,CN} t\}$$

$$= \boxed{C_x \cos(\tilde{\omega} t)} + 2C_y N_\gamma \sin(\tilde{\omega} t)$$

$$N_\gamma = N_z \cos\gamma_{PR} - N_y \sin\gamma_{PR}$$

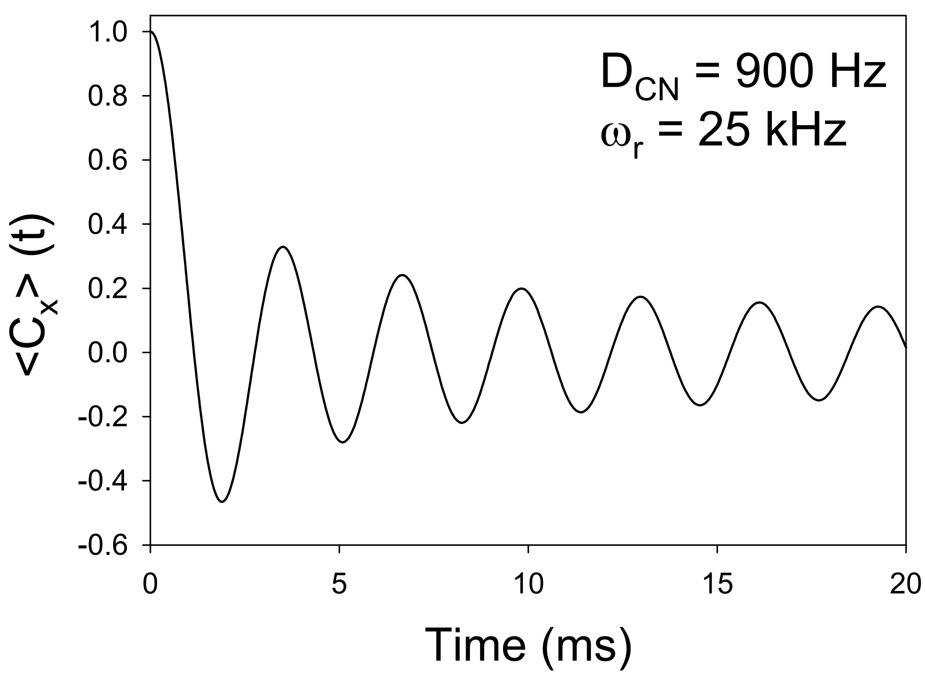

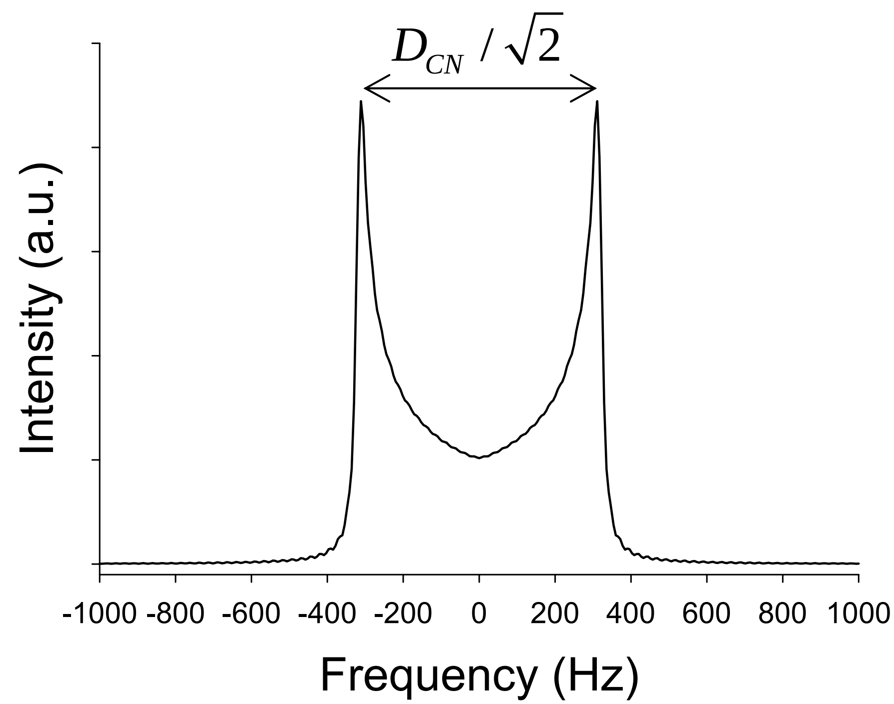

R^3 in Real Systems: Effect of CSA of Irradiated Spin

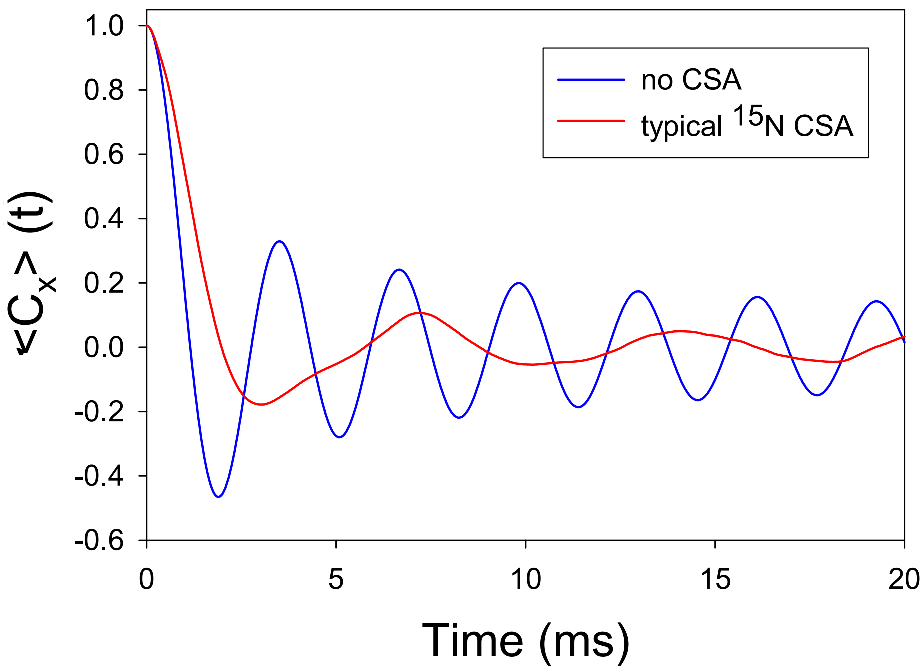

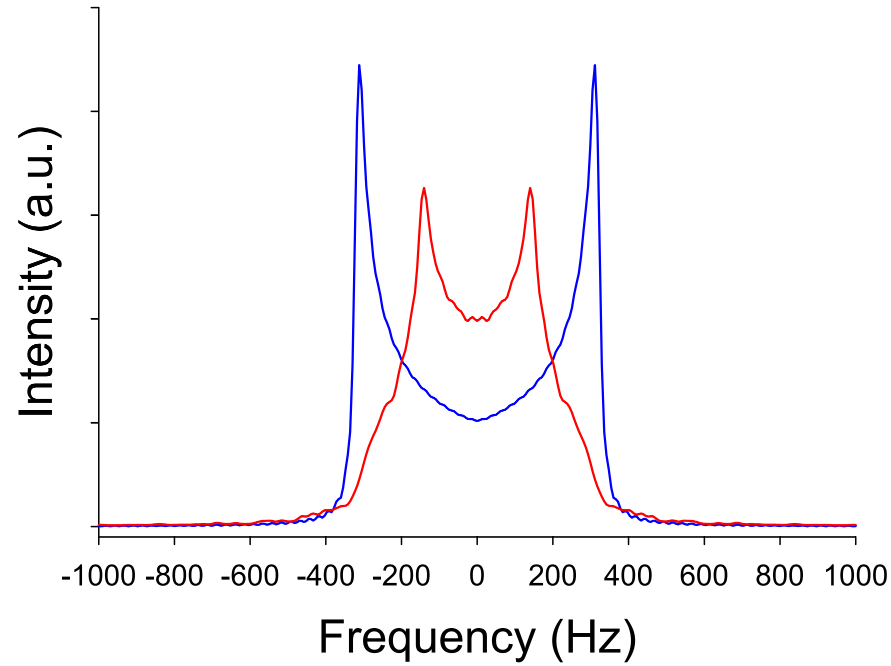

- R^3 also recouples ^{15}N CSA, which doesn't commute with dipolar term
- Dipolar dephasing depends on CSA magnitude and orientation: ***problem for quantitative distance measurements***
- In experiments also have to consider effects of RF inhomogeneity

Rotational Echo Double Resonance (REDOR)

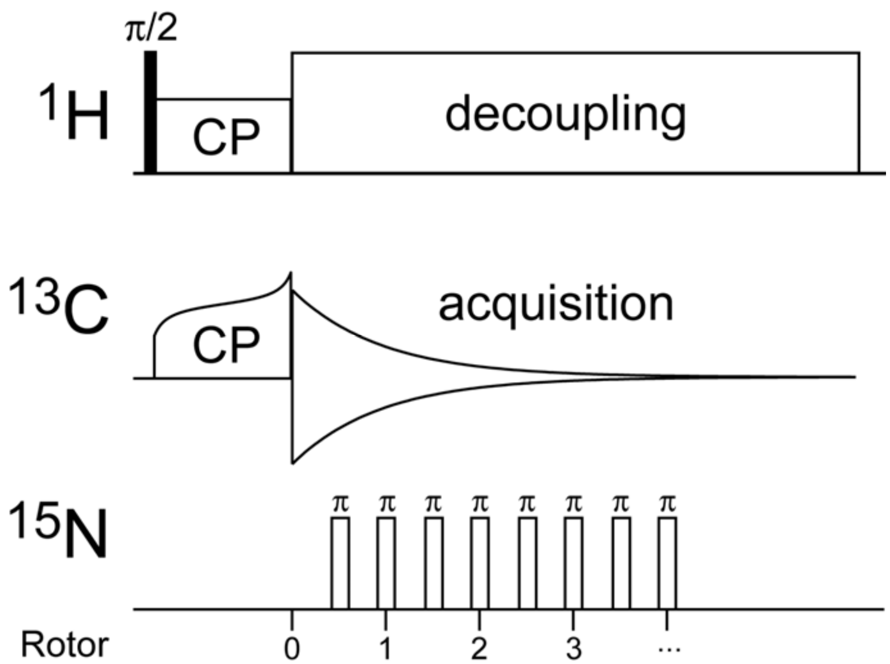

- Apply a series of rotor-synchronized π pulses (2 per τ_r) to ^{15}N spins (this is usually called a dephasing or S experiment)

- Typically a reference (or S_0) experiment with pulses turned off is also, acquired – normally report S/S_0 ratio (or $\Delta S/S_0 = 1 - S/S_0$)

Gullion & Schaefer, JMR 1989

REDOR: AHT Summary

$$H_{IS}(t) = \omega_{IS}(t) 2I_z S_z = -\tfrac{1}{2} b_{IS} \{\sin^2(\beta)\cos[2(\gamma+\omega_r t)] - \sqrt{2}\sin(2\beta)\cos(\gamma+\omega_r t)\} 2I_z S_z$$

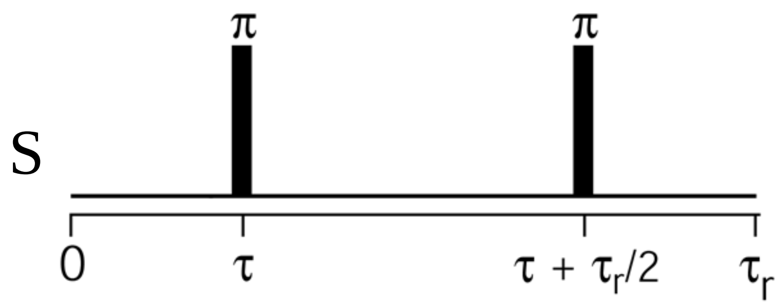

$$\tilde{S}_z = \begin{cases} S_z & 0 < t \le \tau \\ -S_z & \tau < t \le \tau + \tau_r/2 \\ S_z & \tau + \tau_r/2 < t \le \tau_r \end{cases}$$

$$\bar{\tilde{H}}_{IS}^{(0)} = \frac{\sqrt{2}}{\pi} b_{IS} \sin(2\beta)\sin(\gamma+\psi)\cdot 2I_z S_z; \qquad \psi = \omega_r \tau \quad \text{(sequence phase)}$$

$$\bar{\tilde{H}}_{IS}^{(0)} = \begin{cases} -\dfrac{\sqrt{2}}{\pi} b_{IS} \sin(2\beta)\sin(\gamma)\cdot 2I_z S_z & \text{for } \tau = \tau_r/2 \\ \dfrac{\sqrt{2}}{\pi} b_{IS} \sin(2\beta)\sin(\gamma)\cdot 2I_z S_z & \text{for } \tau = 0 \end{cases}$$

- Effective Hamiltonian changes sign as a function of position of pulses within the rotor cycle (must be careful about this in some implementations of REDOR)

REDOR: Typical Implementation

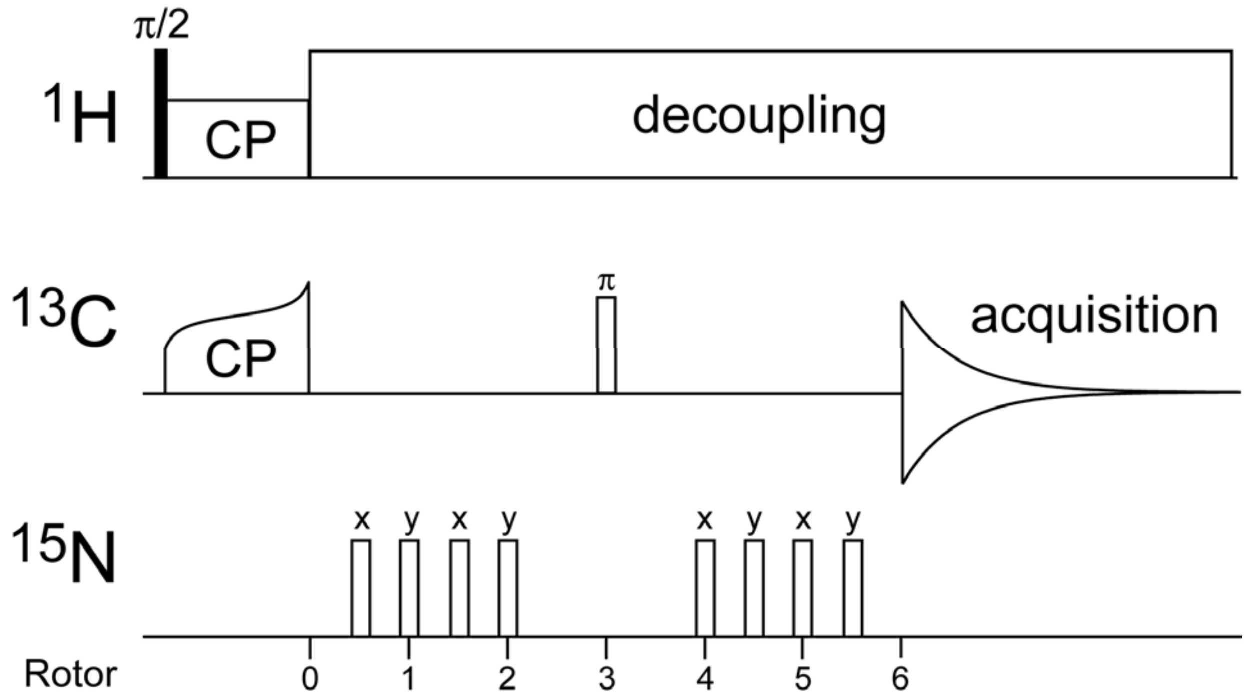

- Rotor synchronized spin-echo on ^{13}C channel refocuses ^{13}C isotropic chemical shift and CSA evolution

- 2nd group of pulses moved by -τ_r/2 relative to 1st group to change sign of H_D and avoid refocusing the ^{13}C-^{15}N dipolar coupling

- xy-type phase cycling of ^{15}N pulses is critical (***Gullion, JMR 1990***)

REDOR Dipolar Evolution

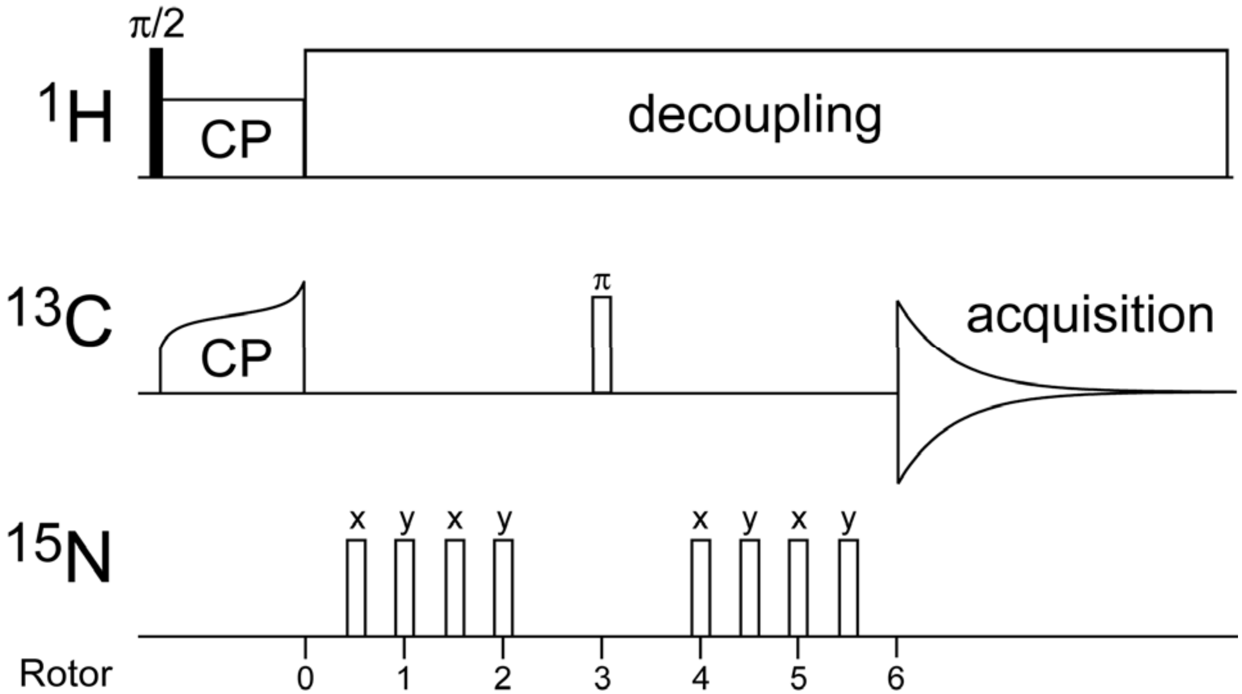

$$\rho(t) = \exp\{-i\tilde{\omega}2C_z N_z t\} C_x \exp\{i\tilde{\omega}2C_z N_z t\}$$

$$= C_x \cos(\tilde{\omega}t) + 2C_y N_z \sin(\tilde{\omega}t)$$

$$\tilde{\omega} = -\frac{\sqrt{2}}{\pi} b_{IS} \sin(2\beta)\sin(\gamma)$$

REDOR: Example

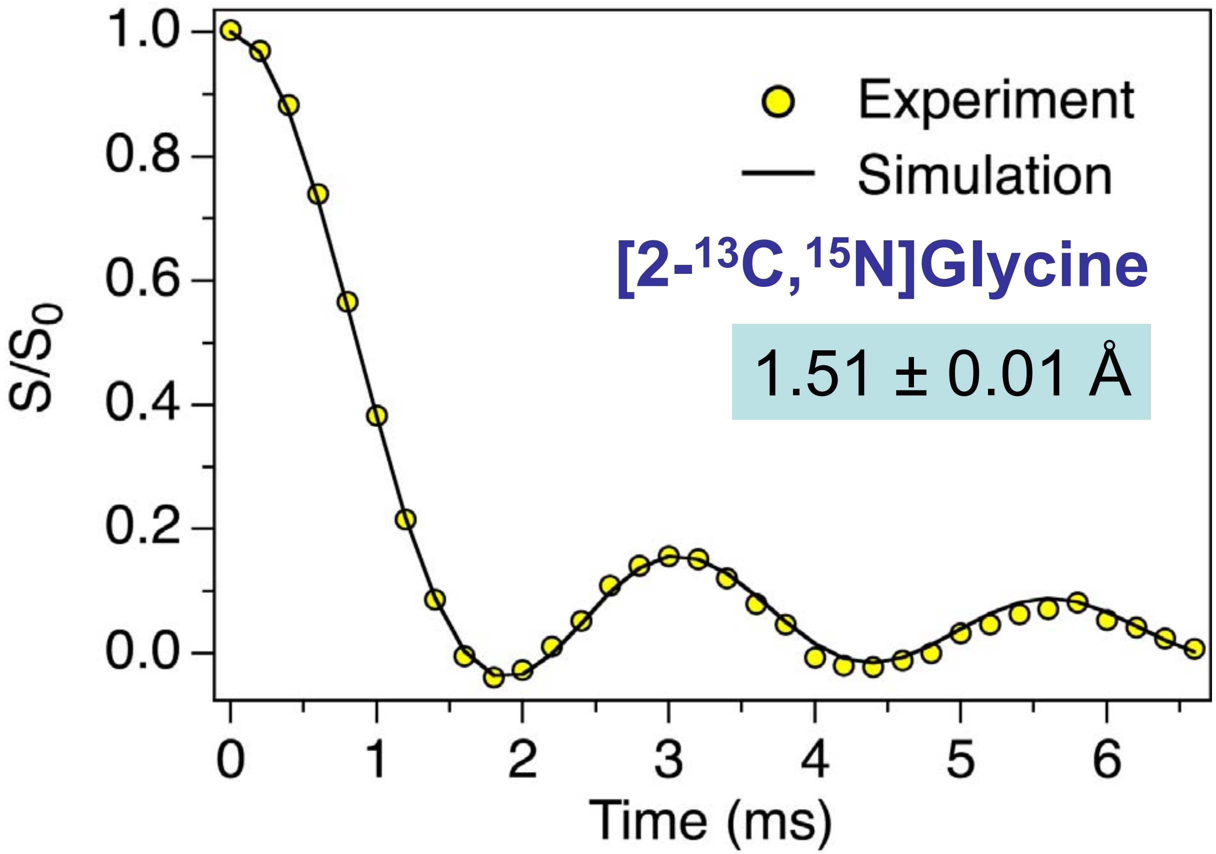

- Experiment highly robust toward ^{15}N CSA, experimental imperfections, resonance offset and finite pulse effects (**xy-4/xy-8 phase cycling is critical for this**)

- REDOR is used routinely to measure distances up to ~5-6 Å (D ~ 25 Hz) in isolated ^{13}C-^{15}N spin pairs

REDOR: More Challenging Case

S112(^{13}C′)-Y114(^{15}N) Distance Measurement in TTR(105-115) Amyloid Fibrils

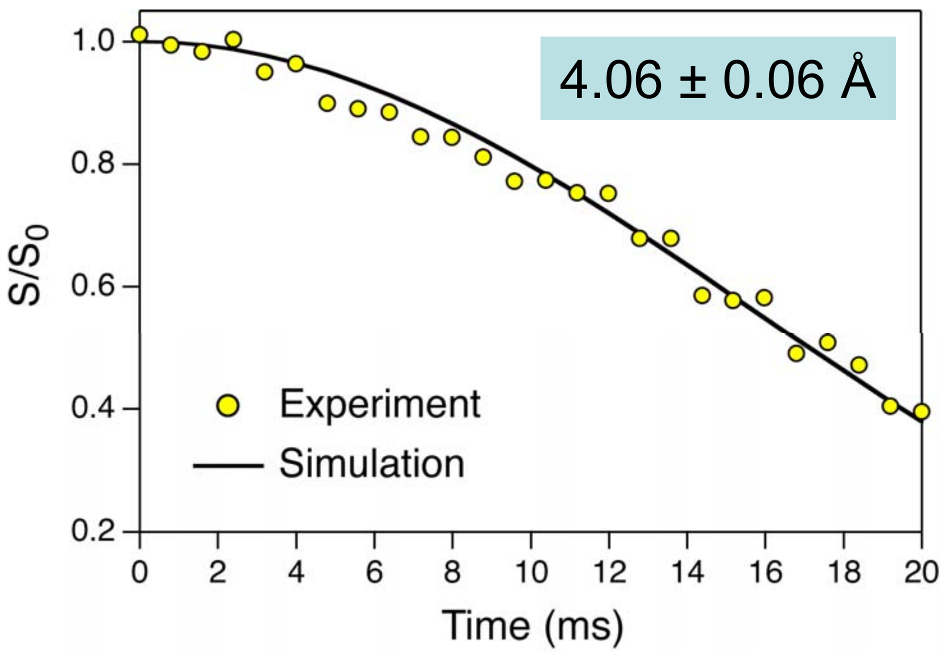

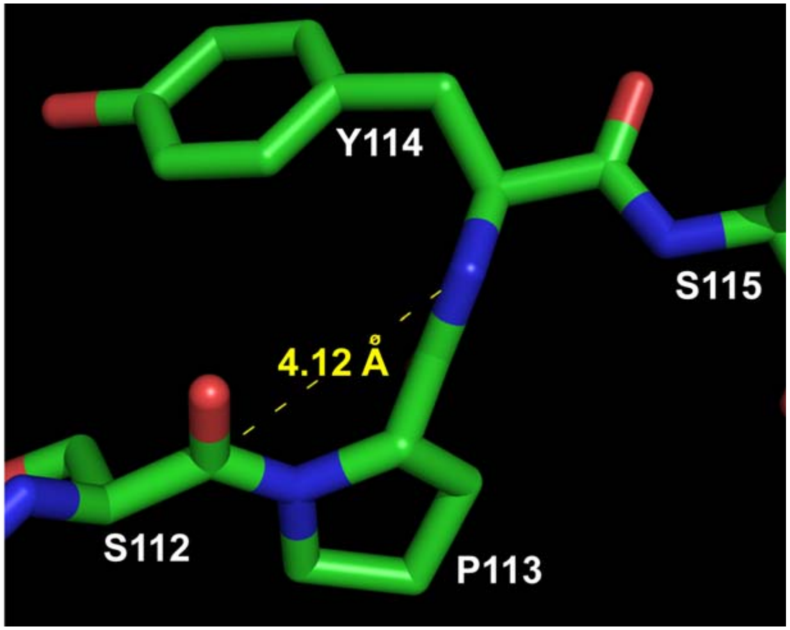

REDOR: ^{15}N CSA Effects

$$xy-4: \quad xyxy$$

Gullion, Baker & Conradi, JMR 1990

$$xy-8: \quad xyxy\ yxyx$$

$$xy-16: \quad xyxy\ yxyx\ \overline{xyxy}\ \overline{yxyx}$$

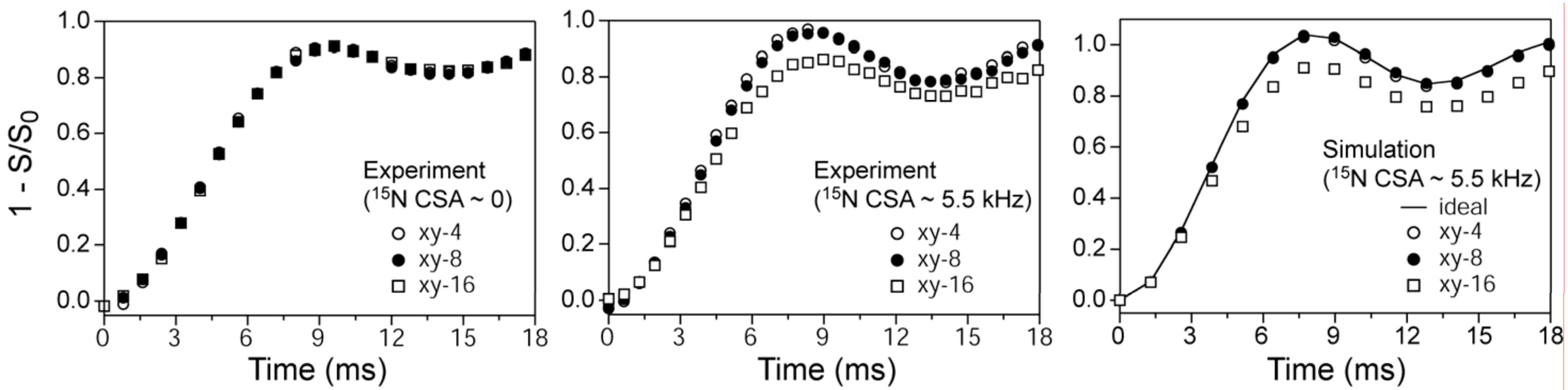

- Simpler schemes (xy-4, xy-8) seem to perform better with respect to ^{15}N CSA compensation than the longer xy-16

- Since $[\overline{H}_D^{(0)}, \overline{H}_{CSA}^{(0)}] = 0$ the behavior is likely due to finite pulses and higher order terms in the average Hamiltonian expansion

REDOR at High MAS Rates

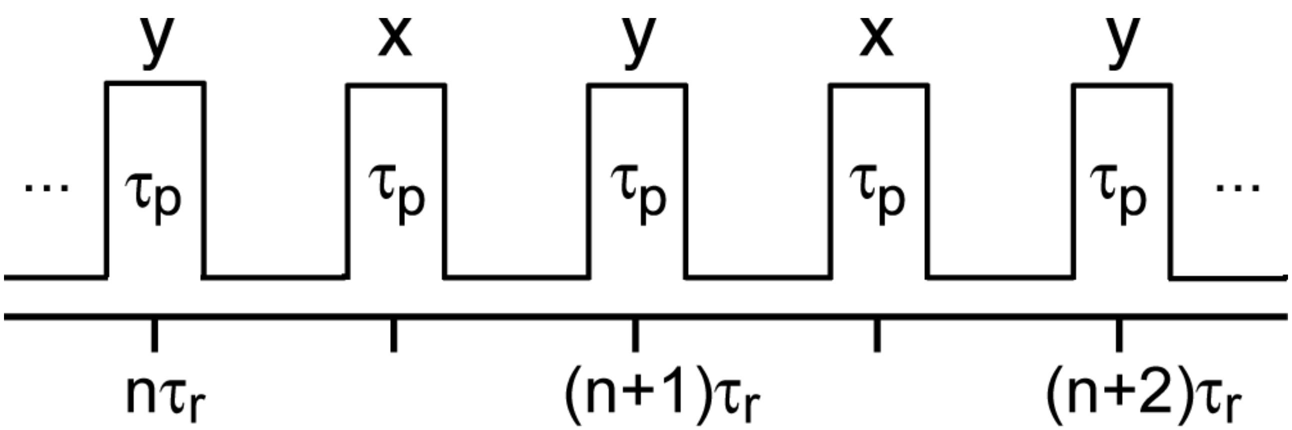

$$\varphi = \frac{2\tau_p}{\tau_r}$$

τ_p (μs)	ν_r (kHz)	φ
10	5	0.1
10	10	0.2
10	20	0.4
20	20	0.8

REDOR (xy-4) at High MAS: AHT

$$\tilde{H}_{IS}(t) = \omega_{IS}(t)\left\{ f(t)2I_zS_z + g(t)2I_zS_x + h(t)2I_zS_y \right\}$$

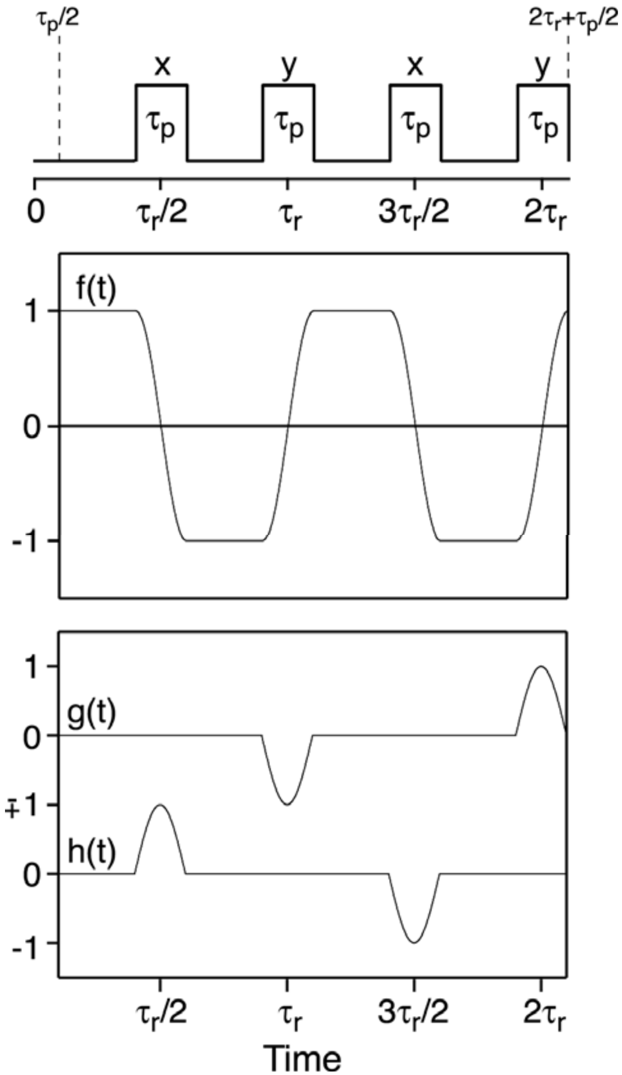

$$\begin{aligned}
\bar{\tilde{H}}_{IS}^{(0)} \propto \frac{1}{\tau_r}\{ & \int_{t_1} (ac'' + bc')dt \cdot 2I_zS_z \\
& + \int_{t_2} (ac'' + bc')\cos[\theta(t)]dt \cdot 2I_zS_z + \int_{t_2} (ac'' + bc')\sin[\theta(t)]dt \cdot 2I_zS_y \\
& - \int_{t_3} (ac'' + bc')dt \cdot 2I_zS_z \\
& - \int_{t_4} (ac'' + bc')\cos[\theta(t)]dt \cdot 2I_zS_z - \int_{t_4} (ac'' + bc')\sin[\theta(t)]dt \cdot 2I_zS_x \\
& + \int_{t_5} (ac'' + bc')dt \cdot 2I_zS_z \\
& + \int_{t_6} (ac'' + bc')\cos[\theta(t)]dt \cdot 2I_zS_z - \int_{t_6} (ac'' + bc')\sin[\theta(t)]dt \cdot 2I_zS_y \\
& - \int_{t_7} (ac'' + bc')dt \cdot 2I_zS_z \\
& - \int_{t_8} (ac'' + bc')\cos[\theta(t)]dt \cdot 2I_zS_z + \int_{t_8} (ac'' + bc')\sin[\theta(t)]dt \cdot 2I_zS_x \}
\end{aligned}$$

Jaroniec et al, JMR 2000

REDOR (xy-4) at High MAS: AHT

$$\bar{\tilde{H}}_{IS}^{(0)} = \begin{cases} -\dfrac{\sqrt{2}}{\pi} b_{IS} \dfrac{\cos\left(\frac{\pi}{2}\varphi\right)}{1-\varphi^2} \sin(2\beta)\sin(\gamma) 2I_z S_z; & \text{finite pulses} \\ -\dfrac{\sqrt{2}}{\pi} b_{IS} \sin(2\beta)\sin(\gamma) 2I_z S_z; & \text{ideal pulses} \end{cases}$$

$$\kappa \equiv \frac{b_{IS}^{eff}}{b_{IS}} = \frac{\cos\left(\frac{\pi}{2}\varphi\right)}{1-\varphi^2}; \qquad \pi/4 \le \kappa \le 1$$

- For xy-4 phase cycling, finite π pulses result only in a simple scaling of the dipolar coupling constant by an additional factor, κ, between $\pi/4$ and 1
- For xx-4 spin dynamics are more complicated and converge to R^3 dynamics in the limit of $\varphi = 1$

REDOR (xy-4) at High MAS: AHT vs. Numerical Simulations

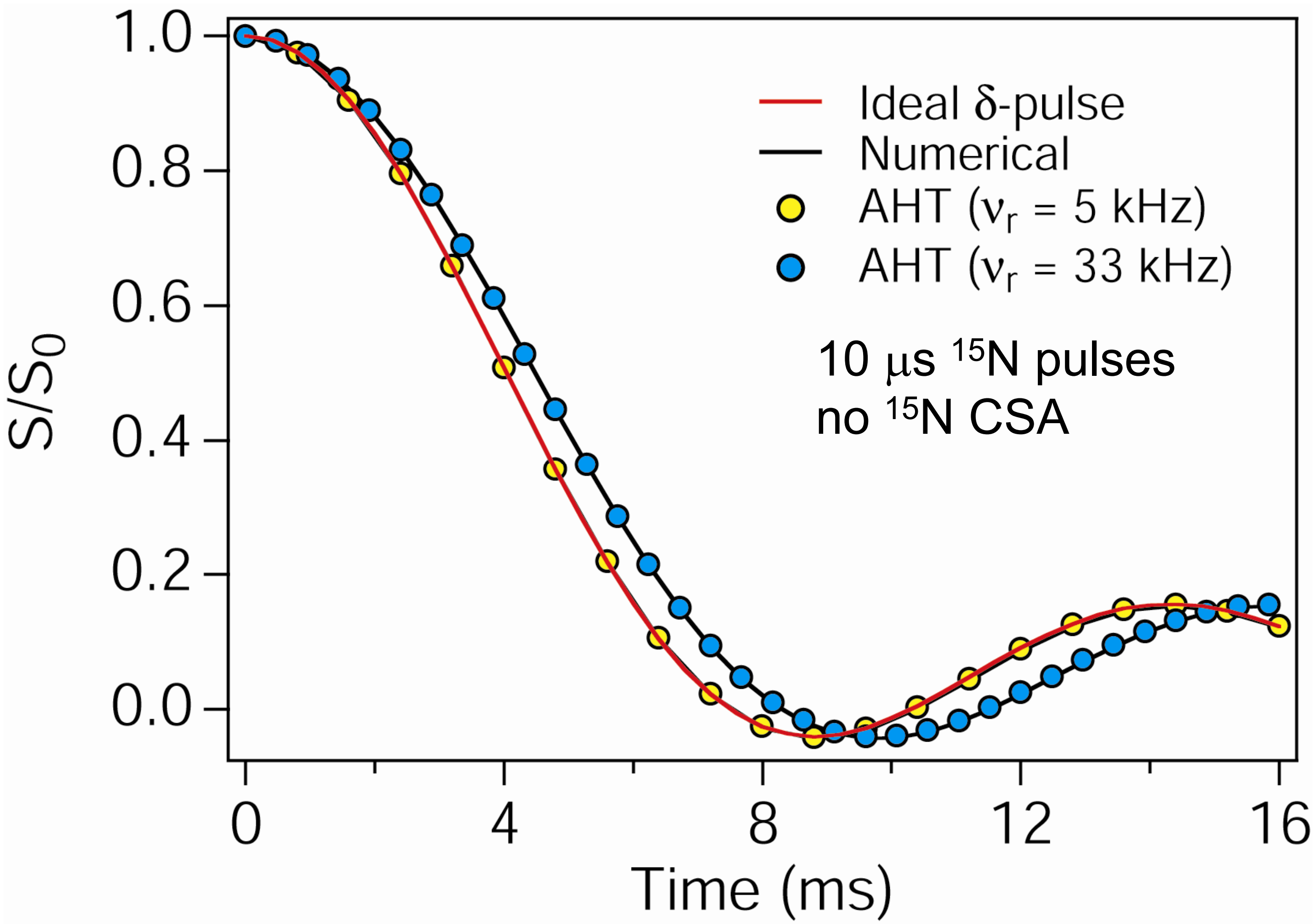

REDOR (xy-4) Experiments

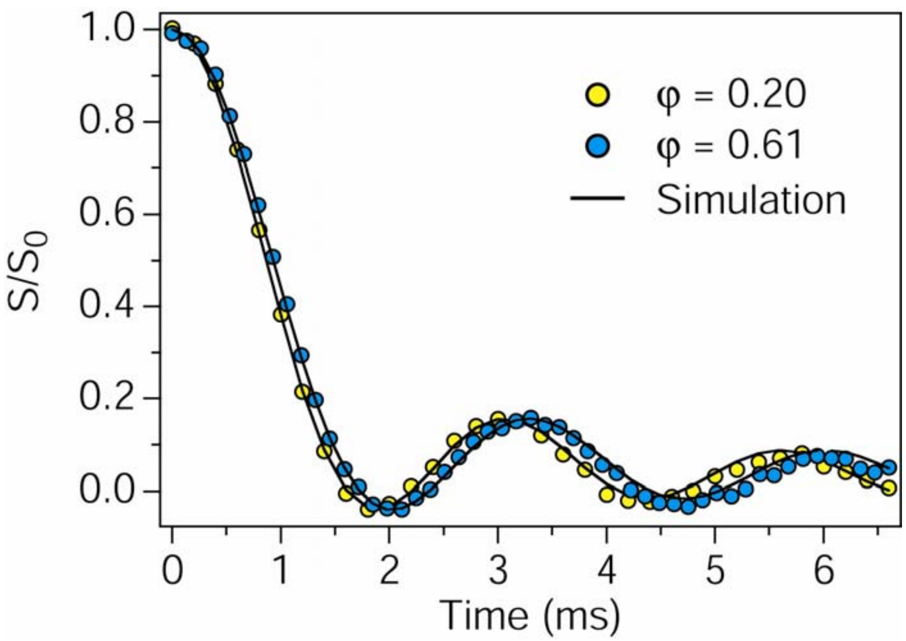

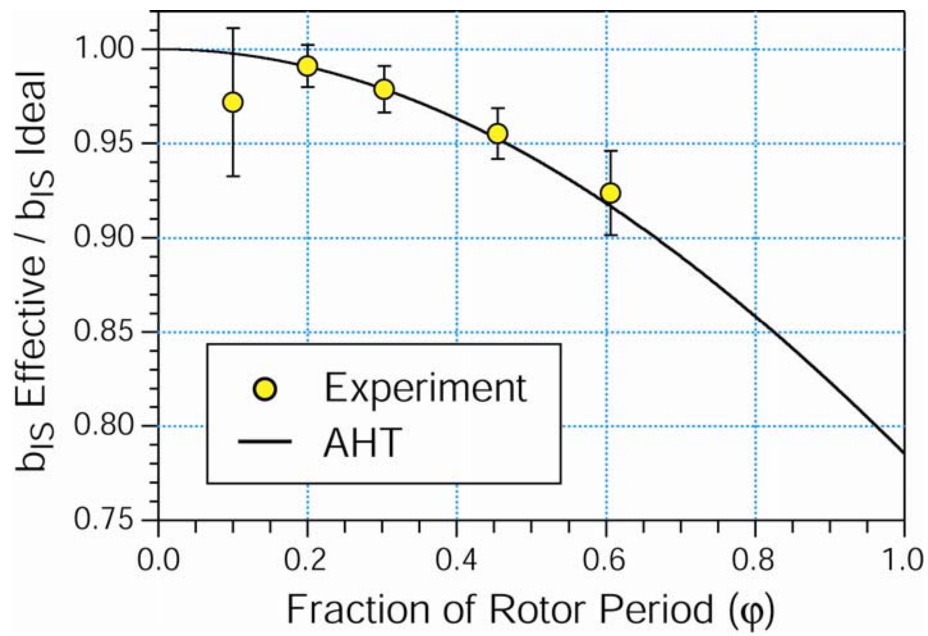

REDOR in Multispin Systems

$$\bar{H}_{IS} = \omega_1 2 I_z S_{1z} + \omega_2 2 I_z S_{2z}$$

$$I_x(t) = \left\langle \cos\left(\omega_1 t\right) \cos\left(\omega_2 t\right) \right\rangle$$

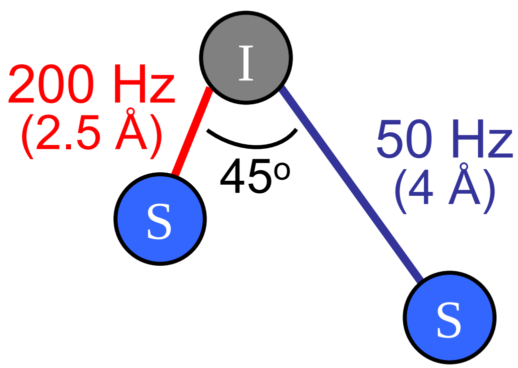

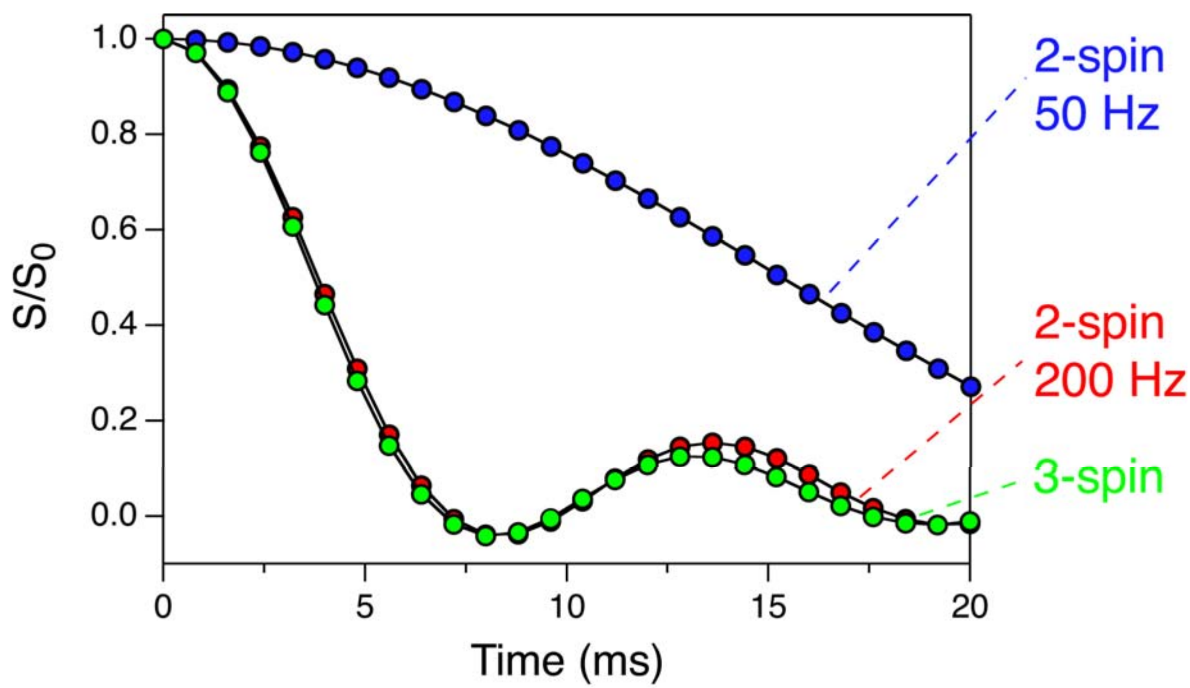

- Strong ^{13}C-^{15}N couplings dominate REDOR dipolar dephasing; weak couplings become effectively ‘invisible’

Frequency Selective REDOR

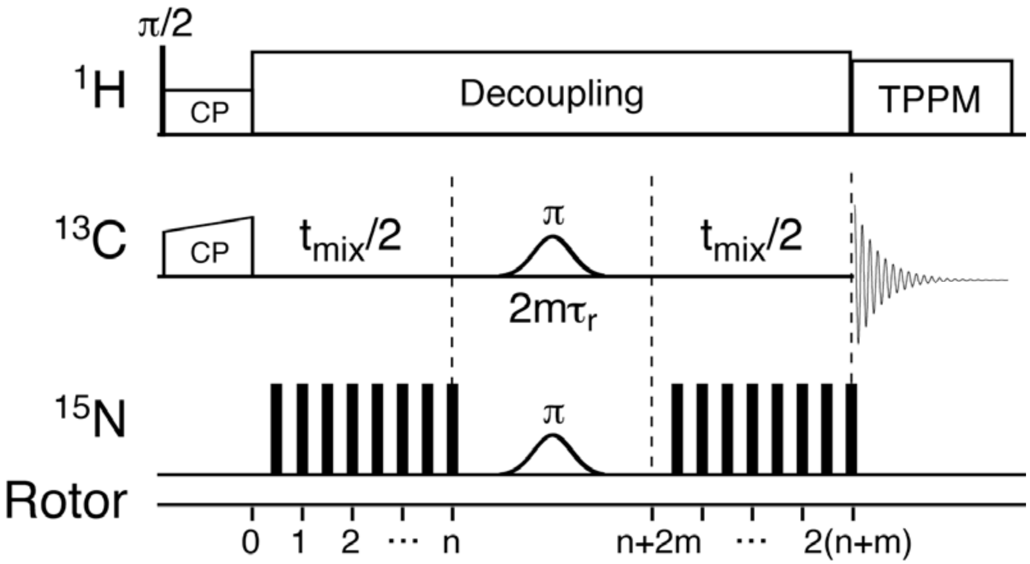

Jaroniec et al, *JACS* 1999, 2001

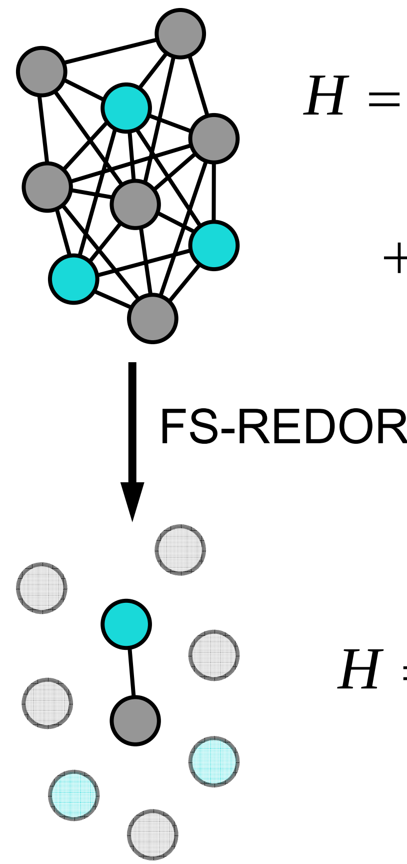

$$H = \sum_{i,j} \omega_{ij} 2I_{iz}S_{jz} + \sum_{i<j} \pi J_{ij} 2I_{iz}I_{jz}$$

$$H = \omega_{kl} 2I_{kz}S_{lz}$$

- Use a pair of weak frequency-selective pulses to ‘isolate’ the ^{13}C-^{15}N dipolar coupling of interest; all other couplings refocused
- This trick is possible because all relevant interactions commute

FS-REDOR Evolution

$$H = H_0 + H_1 + H_2; \qquad [H_0, H_1] = [H_0, H_2] = [H_1, H_2] = 0$$

$$H_0 = \sum_{i \neq k} \sum_{j \neq l} \omega_{ij} 2I_{iz} S_{jz} + \sum_{i<j \neq k} \pi J_{ij} 2I_{iz} I_{jz}; \qquad [H_0, I_{kx}] = [H_0, S_{lx}] = 0$$

$$H_1 = \sum_{i \neq l} \omega_{ki} 2I_{kz} S_{iz} + \sum_{i \neq k} \omega_{il} 2I_{iz} S_{lz} + \sum_{i \neq k} \pi J_{ki} 2I_{kz} I_{iz}; \quad \text{for each term in } H_1 [\ , I_{kx}] \neq 0 \text{ or } [\ , S_{lx}] \neq 0$$

$$H_2 = \omega_{kl} 2I_{kz} S_{lz}; \qquad [H_2, I_{kx}] \neq 0 \text{ and } [H_2, S_{lx}] \neq 0$$

$$U(t) = e^{-iH(t/2)} e^{-i\pi I_{kx}} e^{-i\pi S_{lx}} e^{-iH(t/2)} \overbrace{e^{i\pi S_{lx}} e^{i\pi I_{kx}} e^{-i\pi I_{kx}} e^{-i\pi S_{lx}}}^{\mathbf{1}}$$

$$= e^{-iH(t/2)} e^{-iH_0(t/2)} e^{-iH_2(t/2)} e^{iH_1(t/2)} e^{-i\pi I_{kx}} e^{-i\pi S_{lx}}$$

$$= e^{-iH_0 t} e^{-iH_2 t} e^{-i\pi I_{kx}} e^{-i\pi S_{lx}}$$

$$\rho(0) = I_{kx}; \quad \left[\rho(0), e^{-i\pi S_{lx}}\right] = \left[\rho(0), e^{-i\pi I_{kx}}\right] = \left[\rho(0), e^{-iH_0 t}\right] = 0$$

$$\rho(t) = \boxed{e^{-iH_2 t} I_{kx} e^{iH_2 t}} = \underbrace{I_{kx} \cos(\omega_{kl} t) + 2I_{ky} S_{lz} \sin(\omega_{kl} t)}_{\text{Dipolar evolution under only } b_{kl}}$$

^{13}C Selective Pulses: U-^{13}C Thr

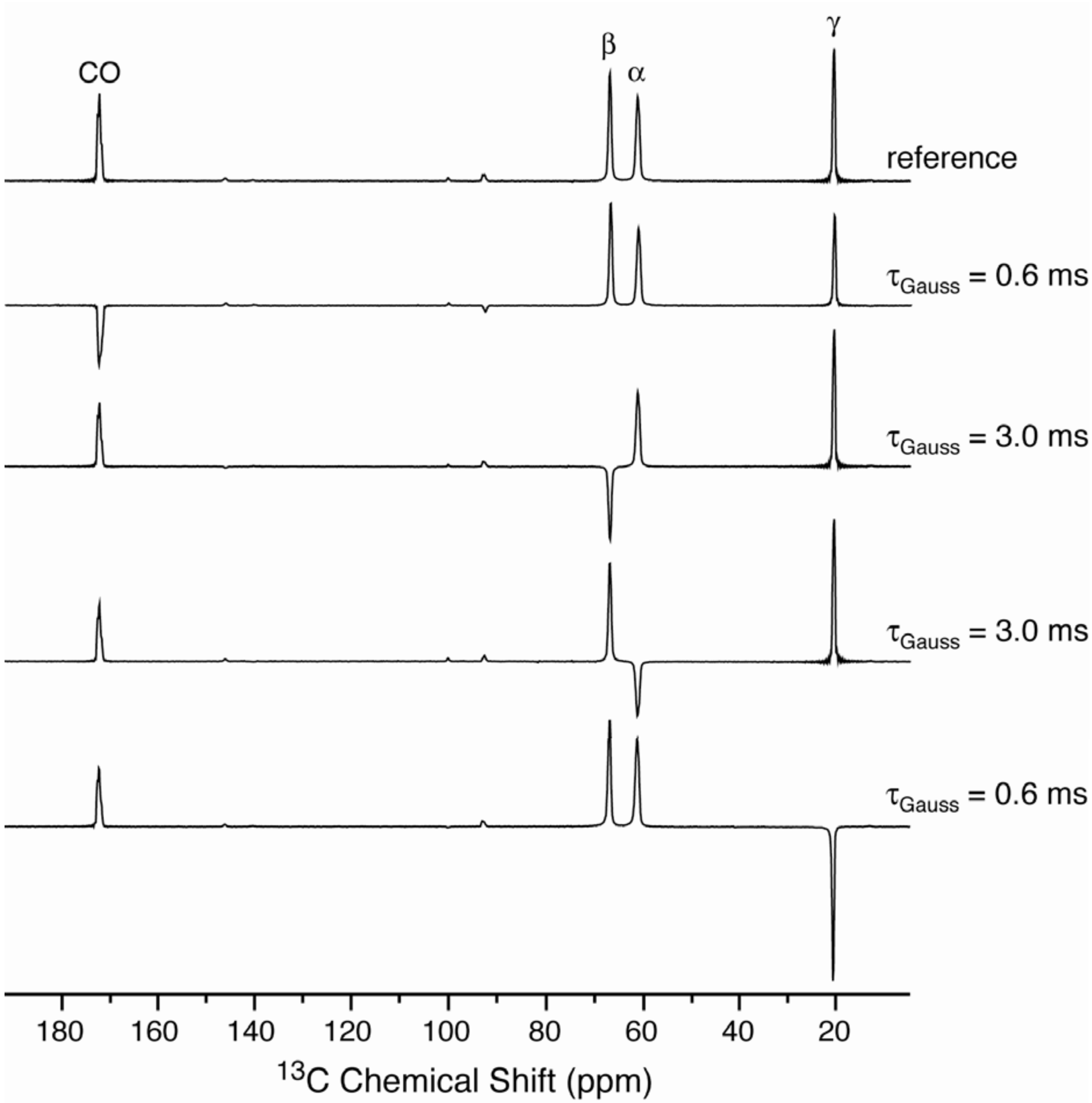

FS-REDOR: U-^{13}C,^{15}N Asn

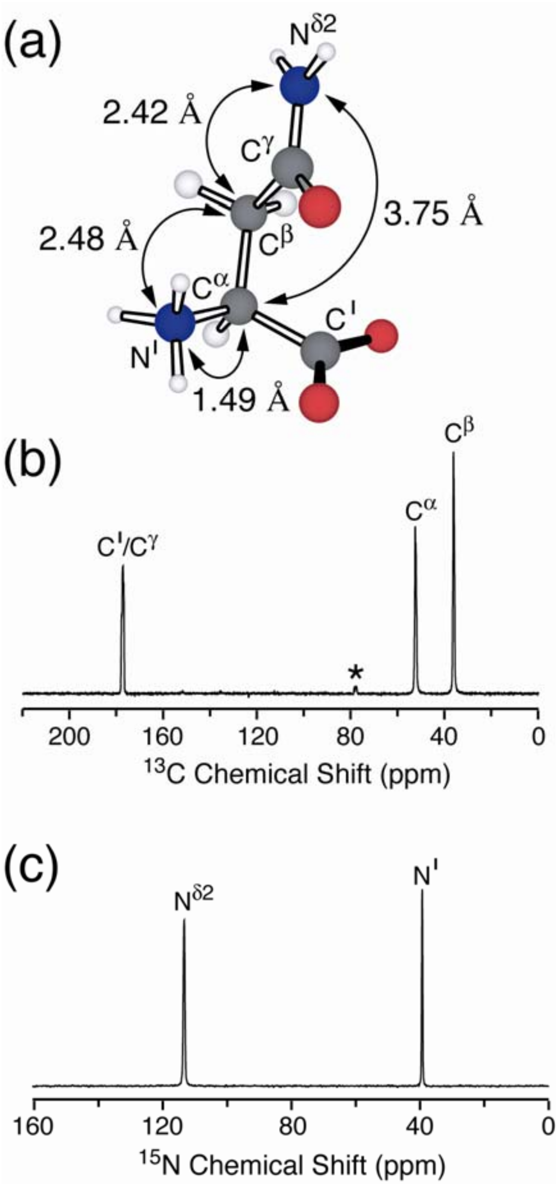

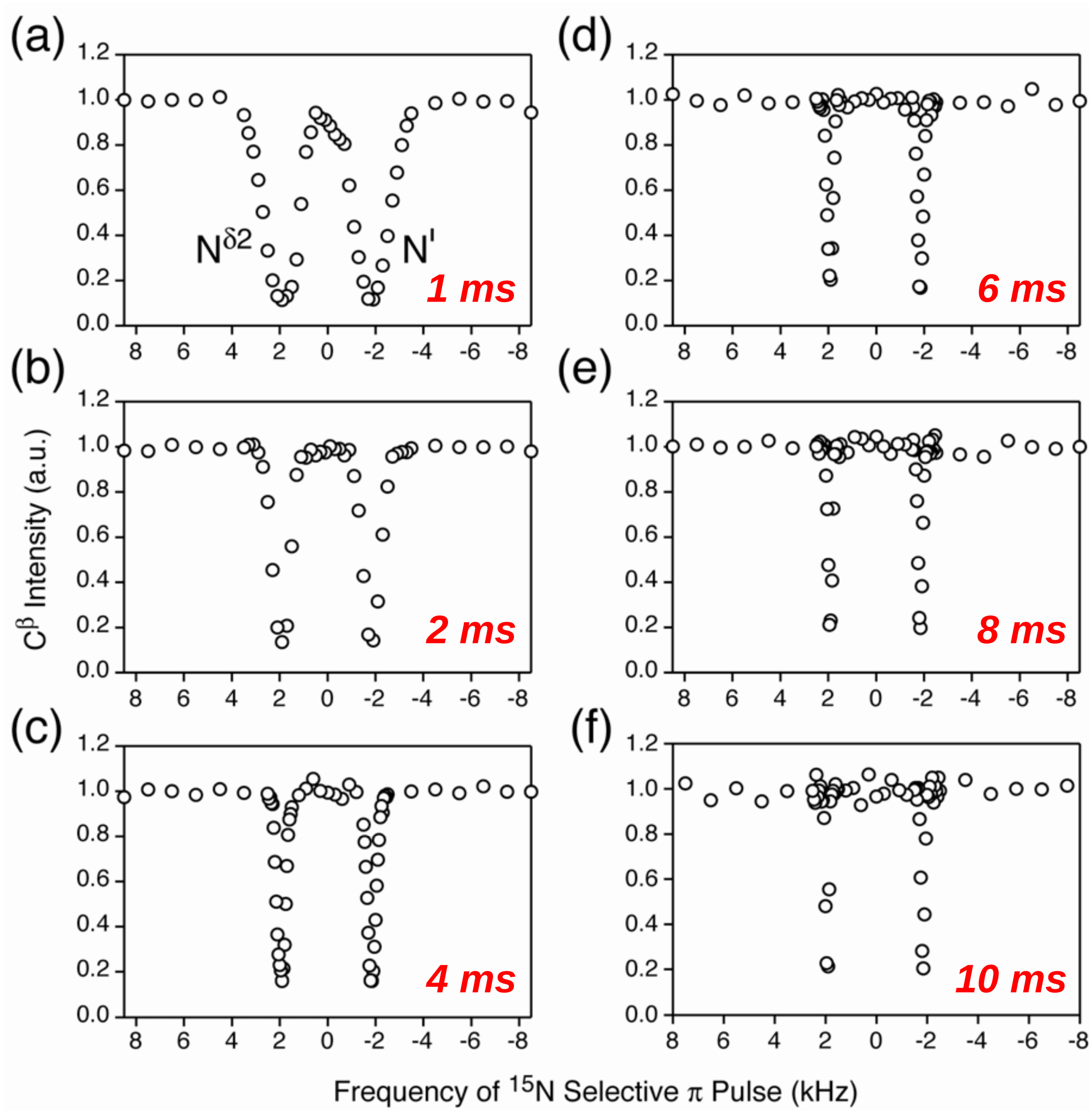

FS-REDOR: U-^{13}C,^{15}N Asn

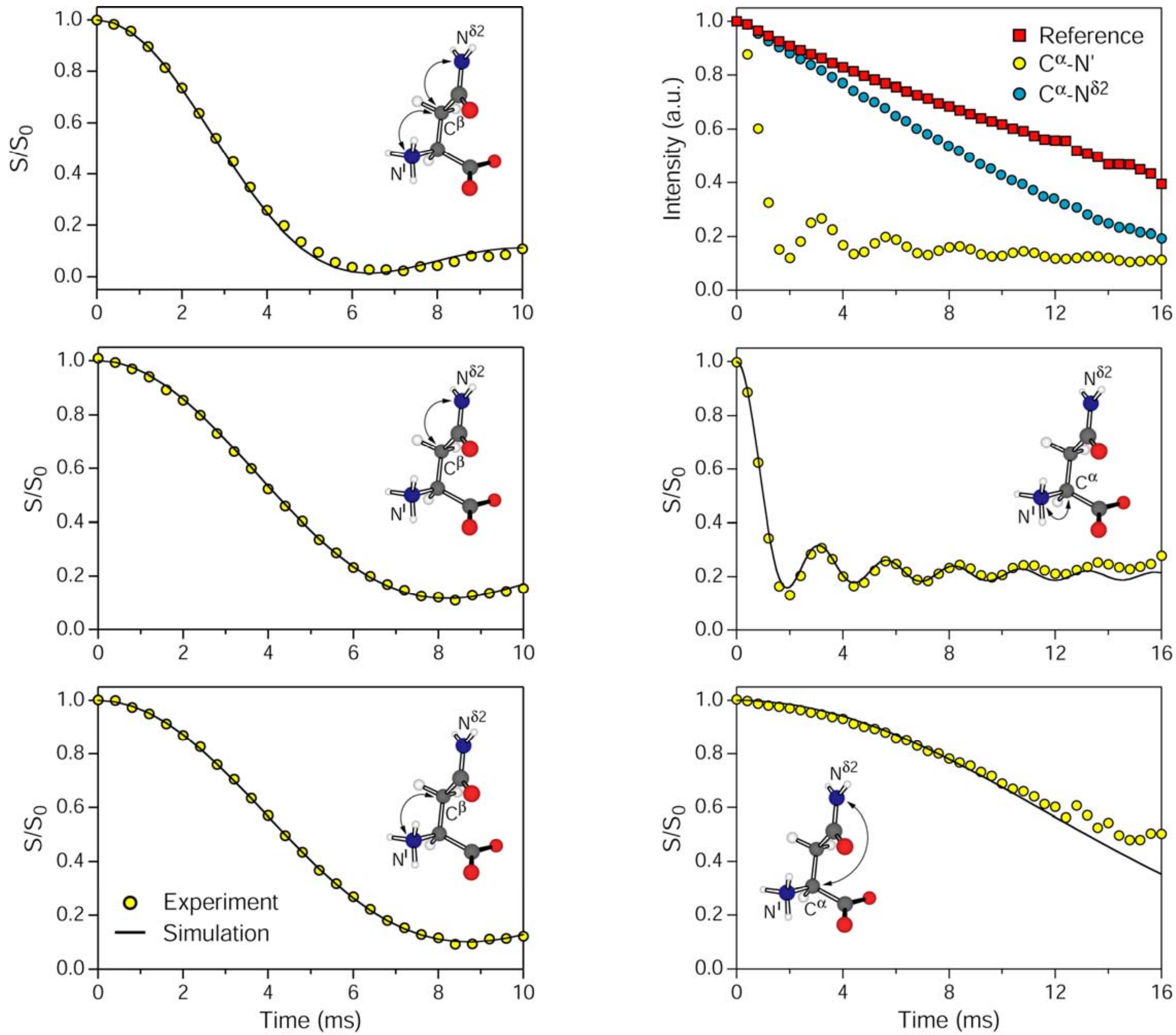

FS-REDOR: U-^{13}C,^{15}N-f-MLF

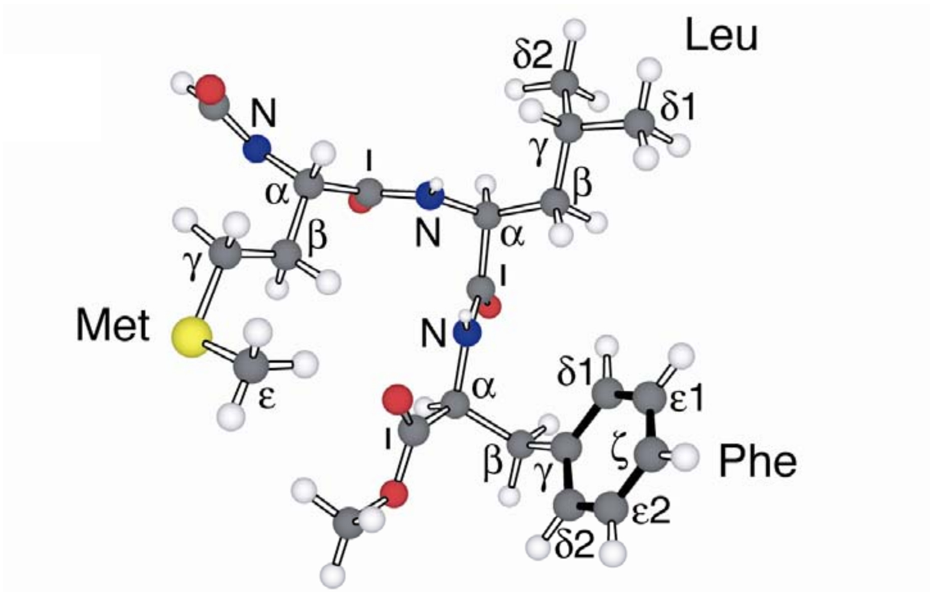

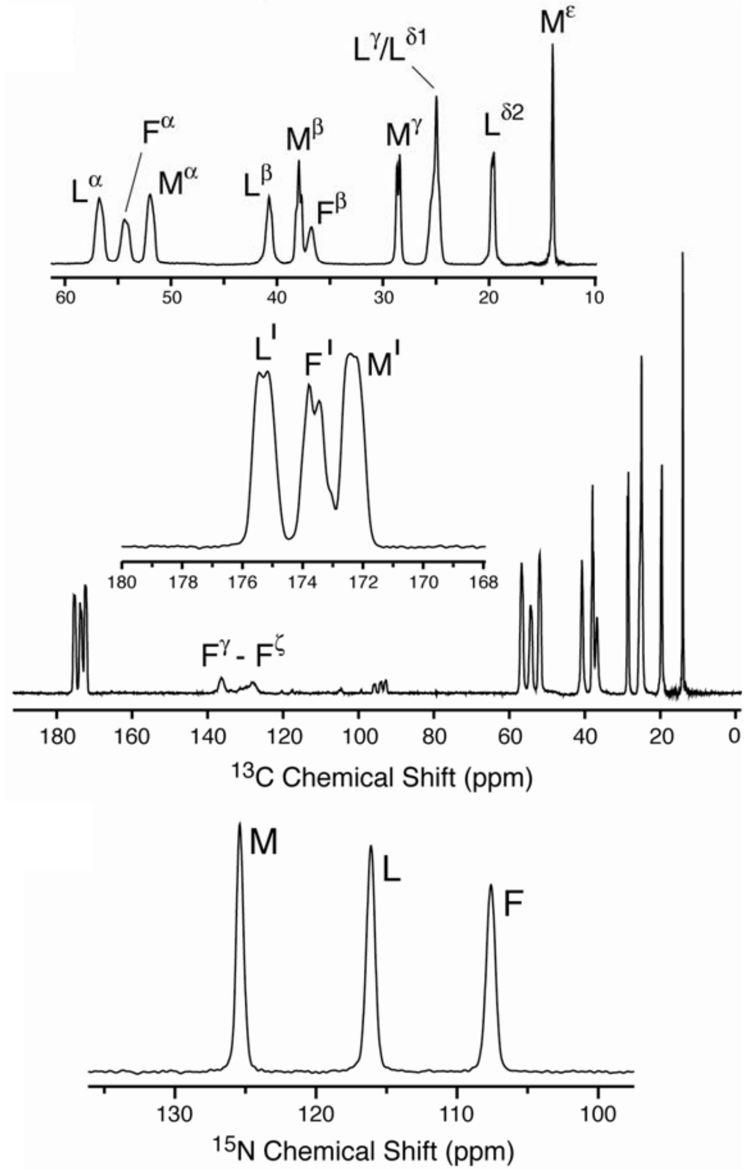

FS-REDOR: U-^{13}C,^{15}N-f-MLF

Leu C$^{\beta}$-Leu N

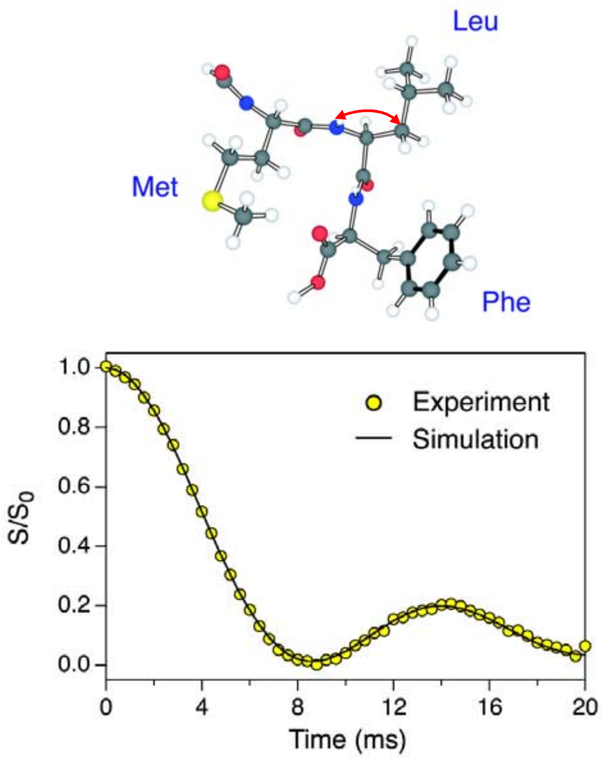

X-ray: 2.50 Å
NMR: 2.46 ± 0.02 Å

Leu C$^{\beta}$-Phe N

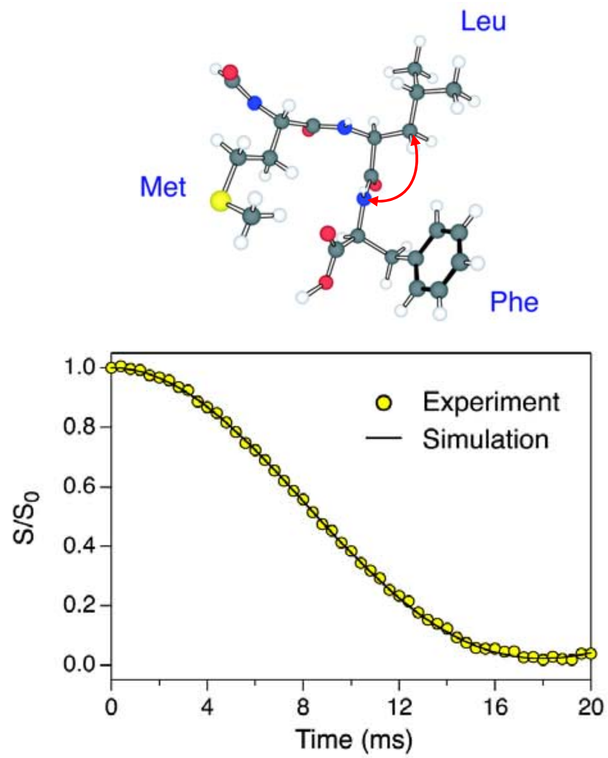

X-ray: 3.12 Å
NMR: 3.24 ± 0.12 Å

Met C$^{\beta}$-Phe N

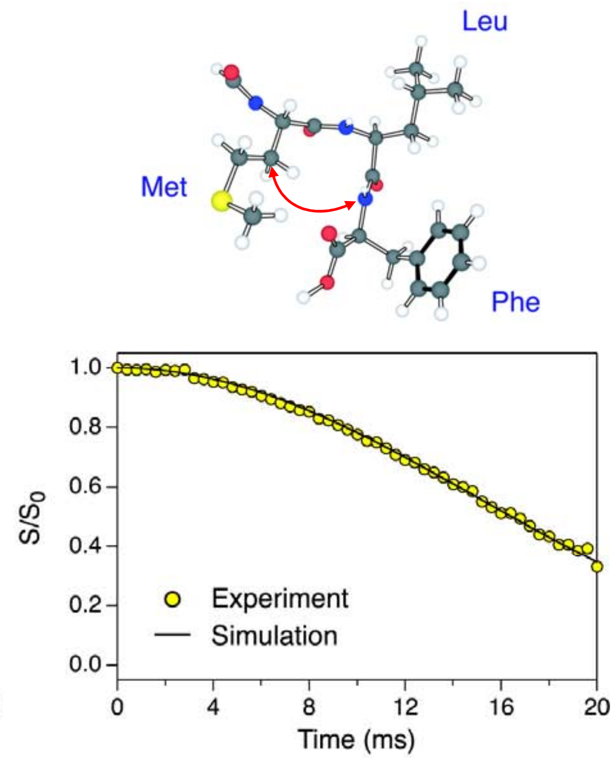

X-ray: 4.06 Å
NMR: 4.12 ± 0.15 Å

FS-REDOR: U-^{13}C,^{15}N-f-MLF

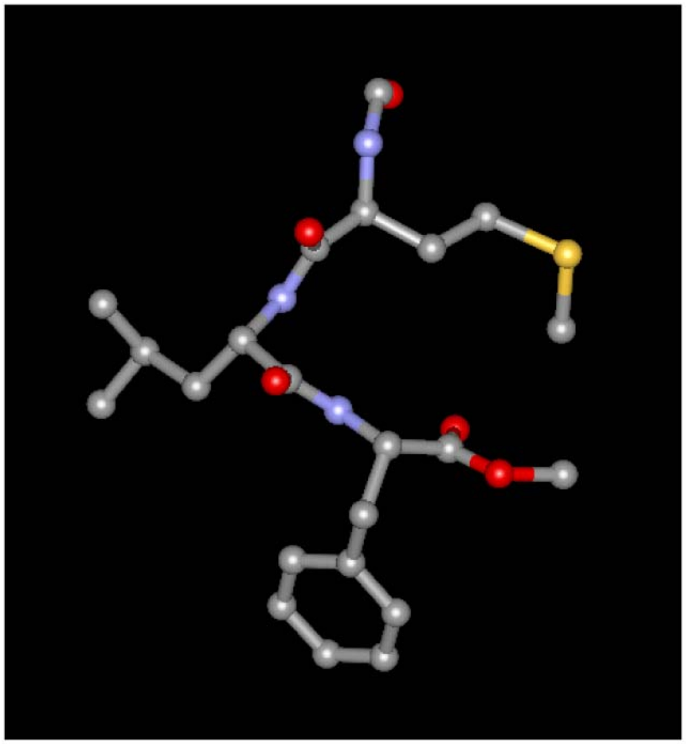

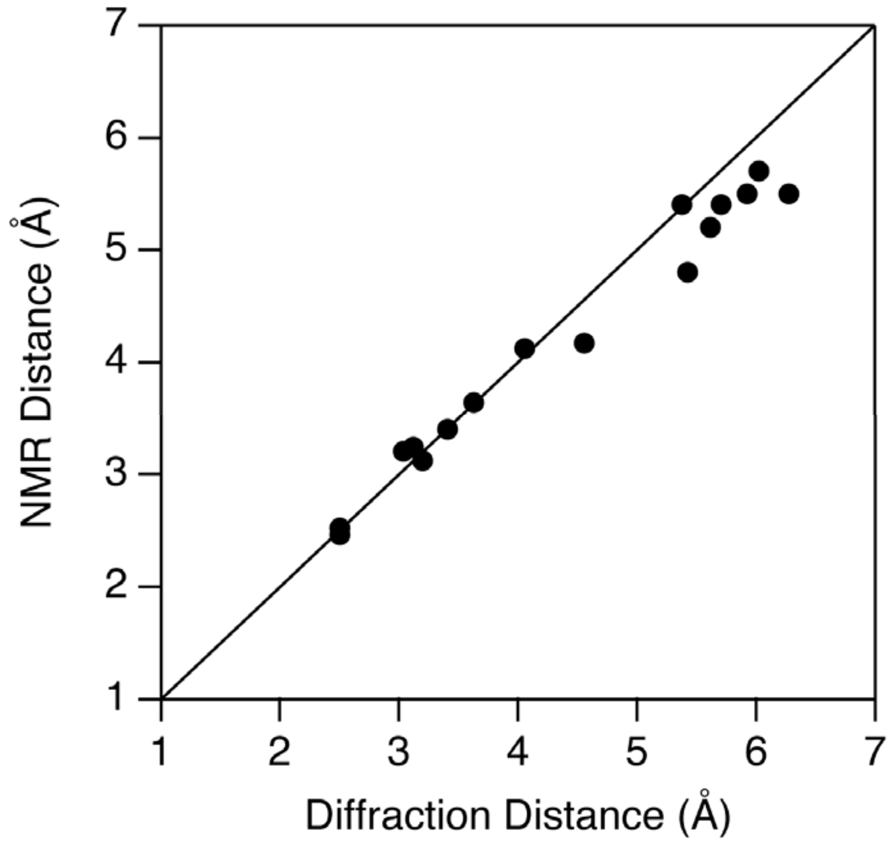

- 16 ^{13}C-^{15}N distances could be measured in MLF tripeptide
- Selectivity of ^{15}N pulse + need of prior knowledge of which distances to probe is a major limitation to U-^{13}C,^{15}N proteins

Simultaneous ^{13}C-^{15}N Distance Measurements in U-^{13}C,^{15}N Molecules

General Pseudo-3D HETCOR (Heteronuclear Correlation) Scheme

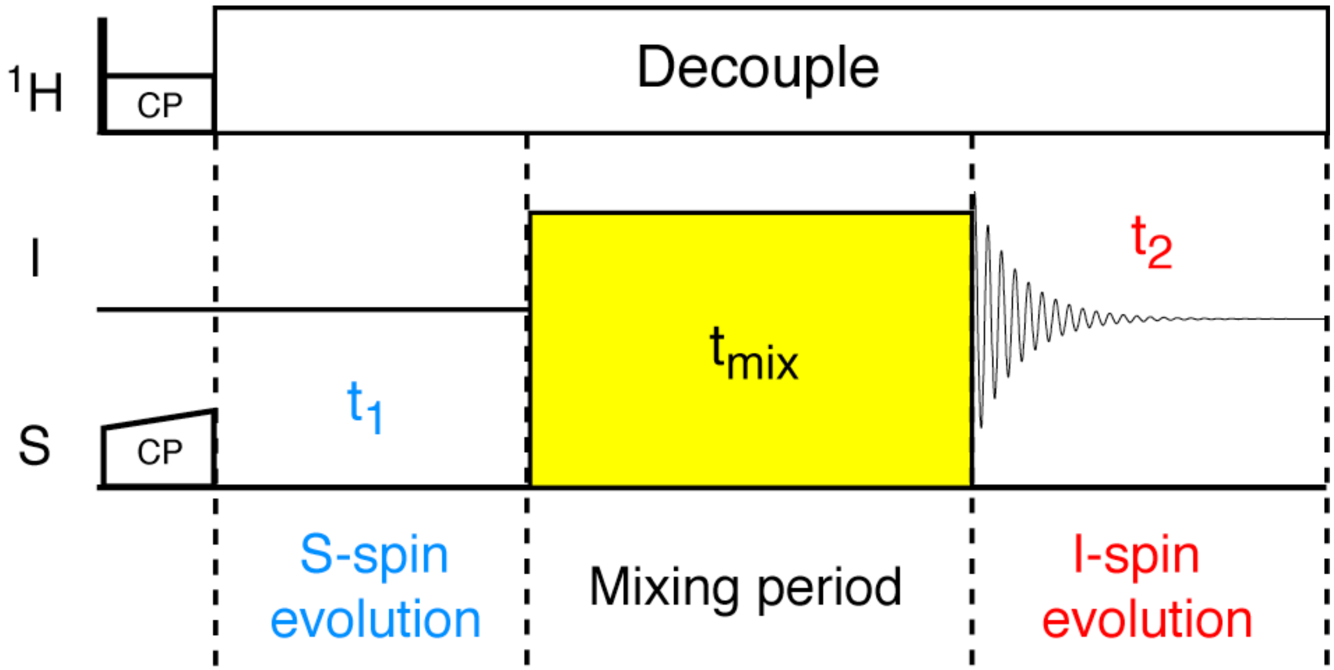

- I-S coherence transfer as function of t_{mix} via D_{IS}
- Identify coupled I and S spins by chemical shift labeling in t_1, t_2

Transferred Echo Double Resonance

3D TEDOR Pulse Sequence

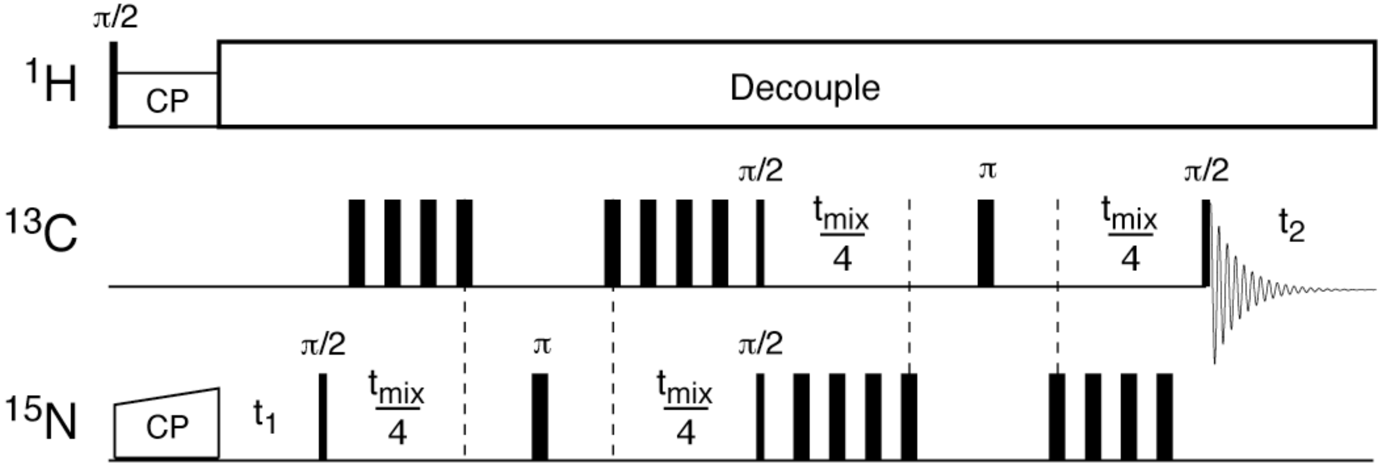

Hing, Vega & Schaefer, *JMR* 1992

$$S_x \xrightarrow{REDOR} 2I_zS_y \sin(\omega_{IS}t_{mix}/2) \xrightarrow{(\pi/2)I_x+(\pi/2)S_x}$$

$$-2I_yS_z \sin(\omega_{IS}t_{mix}/2) \xrightarrow{REDOR} I_x \sin^2(\omega_{IS}t_{mix}/2)$$

- Similar idea to INEPT experiment in solution NMR
- Cross-peak intensities depend on <u>all</u> ^{13}C-^{15}N dipolar couplings
- Experiment not directly applicable to U-^{13}C-labeled samples

3D TEDOR: U-^{13}C,^{15}N Molecules

Modified 3D TEDOR Pulse Sequence

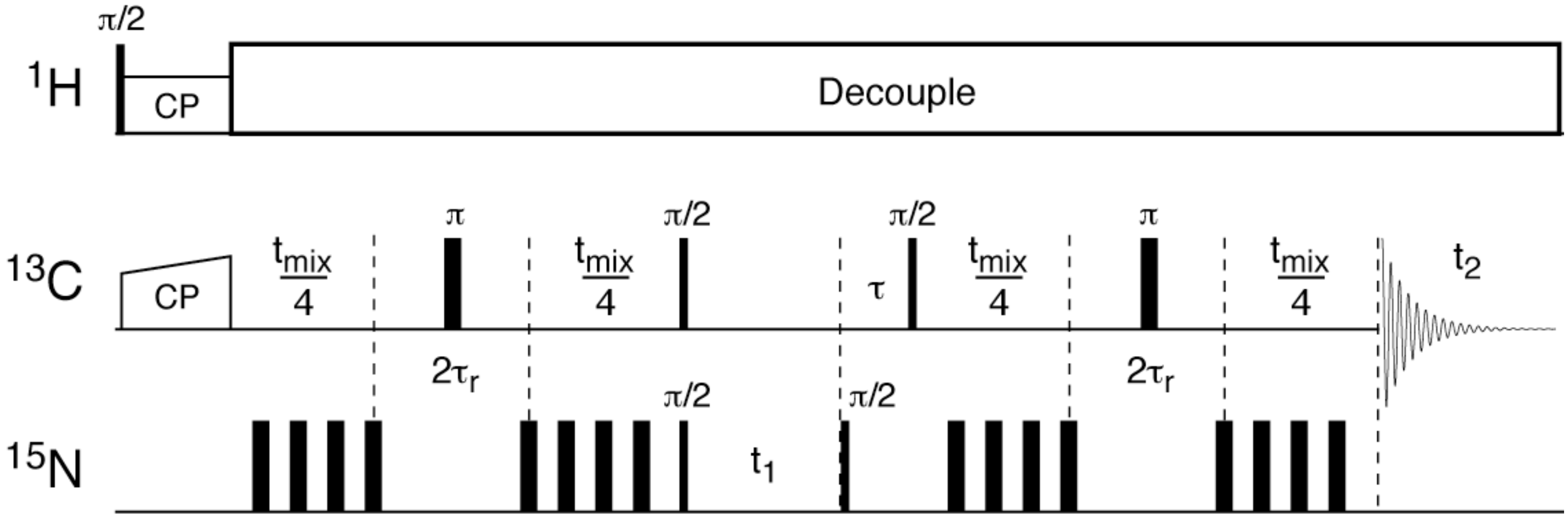

$$I_x \xrightarrow{REDOR} 2I_yS_z \sin(\omega_{IS}t_{mix}/2) \xrightarrow{(\pi/2)S_x+(\pi/2)I_x}$$

$$-2I_zS_y \sin(\omega_{IS}t_{mix}/2) \xrightarrow{(\pi/2)S_x-(\pi/2)I_x}$$

$$-2I_yS_z \sin(\omega_{IS}t_{mix}/2) \xrightarrow{REDOR} I_x \sin^2(\omega_{IS}t_{mix}/2)$$

Michal & Jelinski, *JACS* 1997

3D TEDOR: U-^{13}C,^{15}N Molecules

N-acetyl-Val-Leu

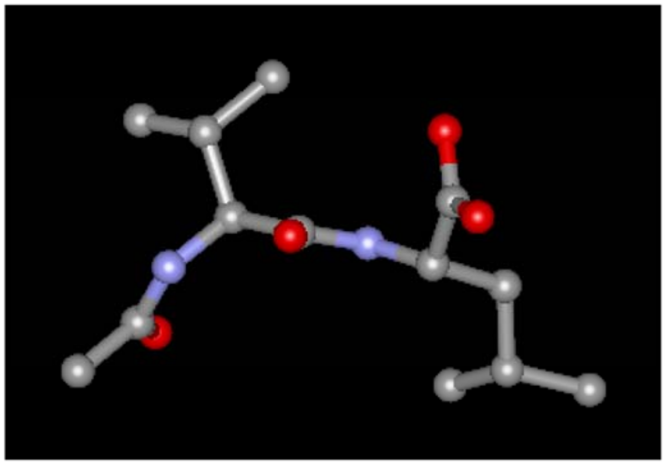

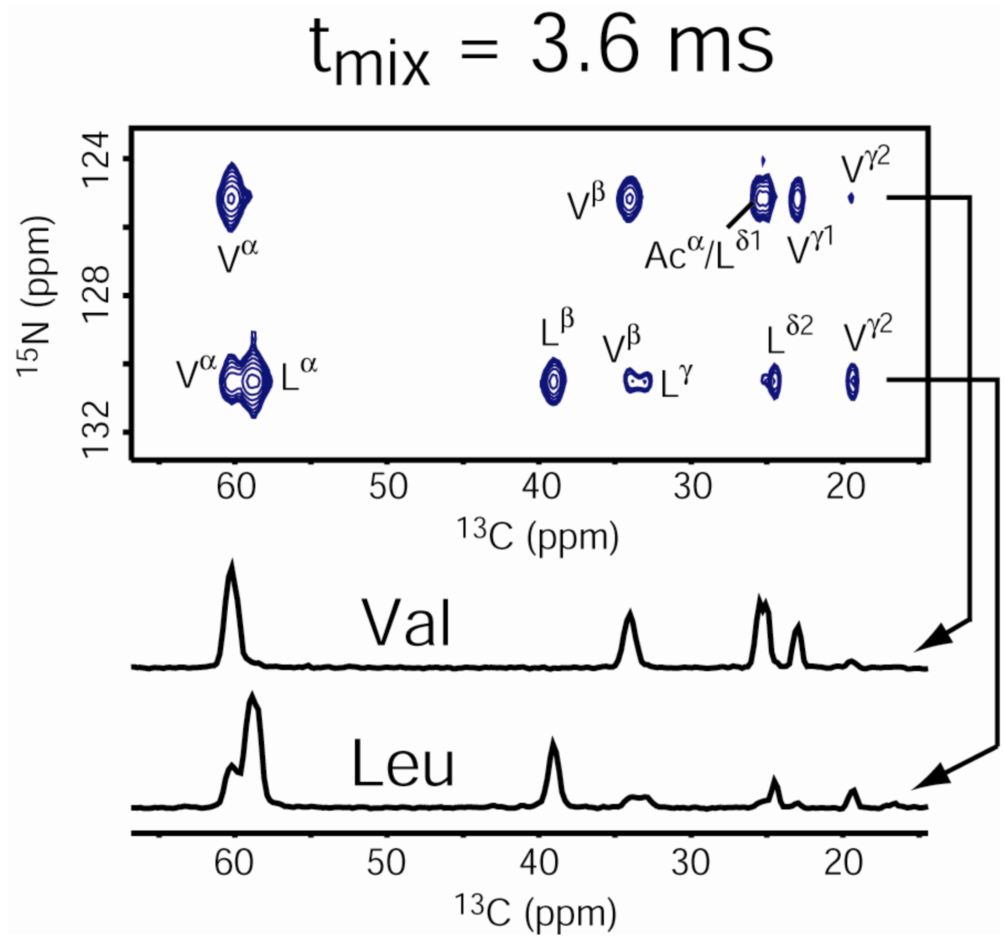

- Cross-peak intensities roughly proportional to ^{13}C-^{15}N dipolar couplings

3D TEDOR: U-^{13}C,^{15}N N-ac-VL

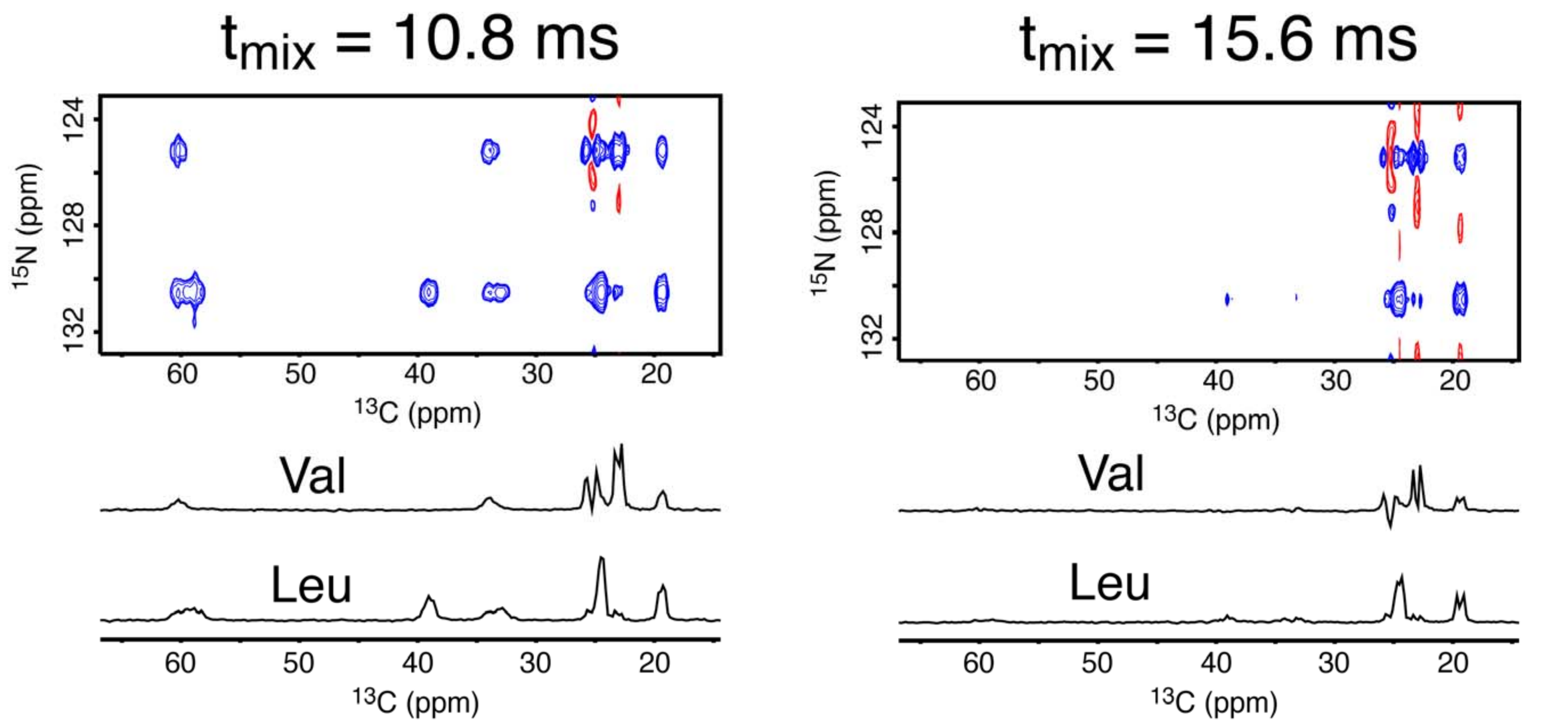

- Spectral artifacts (spurious cross-peaks, phase twisted lineshapes) appear at longer mixing times as result of ^{13}C-^{13}C J-evolution

Improved Scheme: 3D Z-Filtered TEDOR

3D ZF TEDOR Pulse Sequence

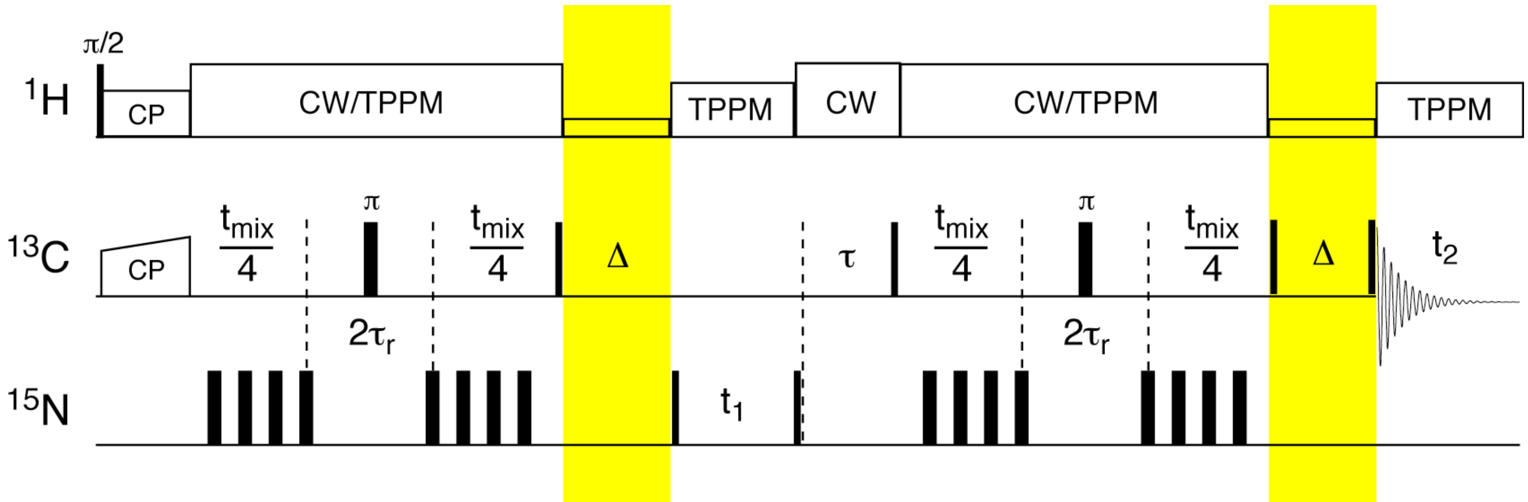

- Unwanted anti-phase and mulitple-quantum coherences responsible for artifacts eliminated using two z-filter periods

Jaroniec, Filip & Griffin, *JACS* 2002

Results in N-ac-VL

3D TEDOR

t_{mix} = 10.8 ms

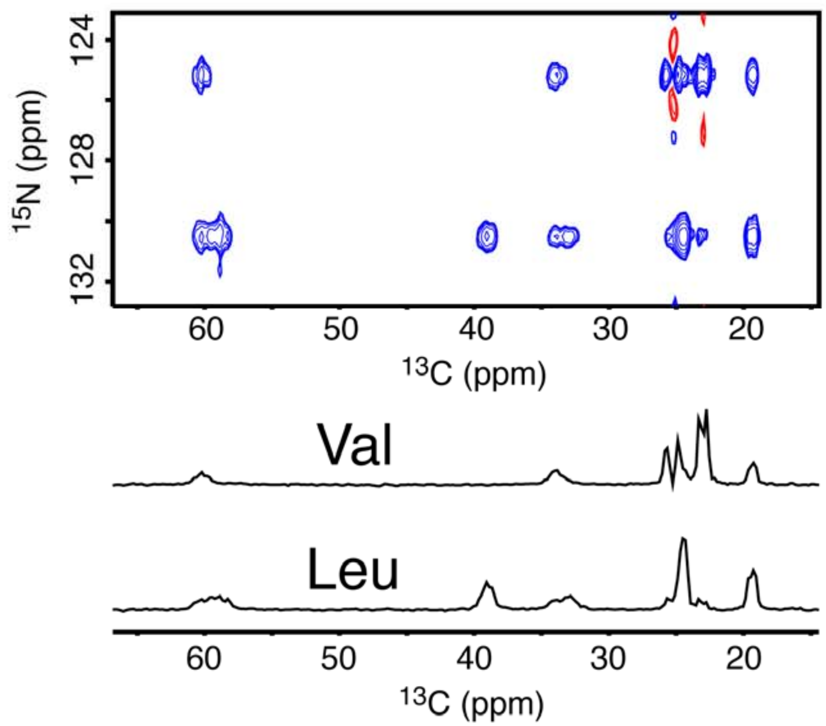

3D ZF TEDOR

t_{mix} = 10.8 ms

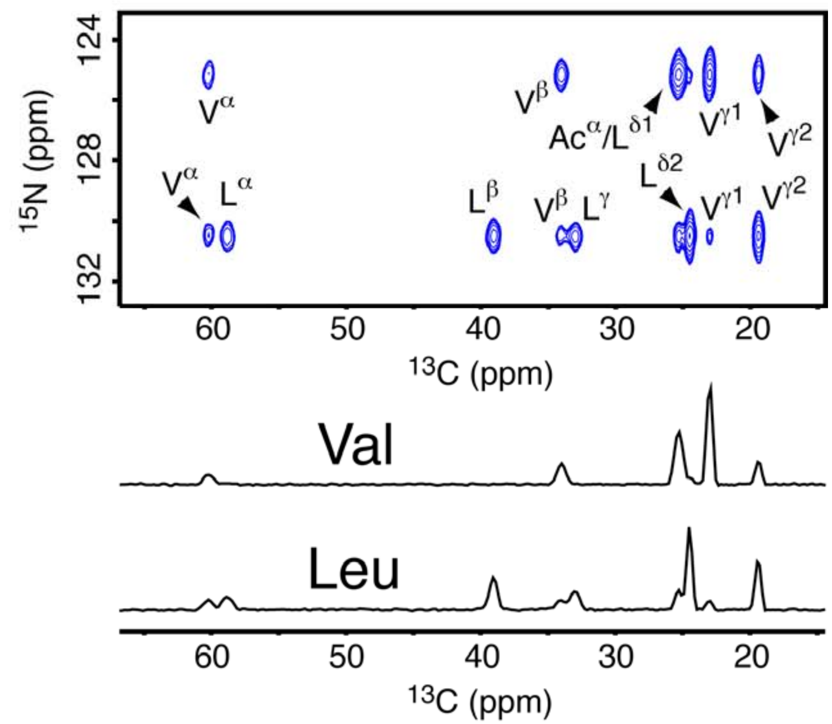

- 3D ZF TEDOR generates purely absorptive 2D spectra
- Cross-peak intensities give qualitative distance information

^{13}C-^{13}C J-Evolution Effects: ZF-TEDOR

Simulated ^{13}C Cross-Peak Buildup
4 Å C-N Distance (D_{CN} = 50 Hz)

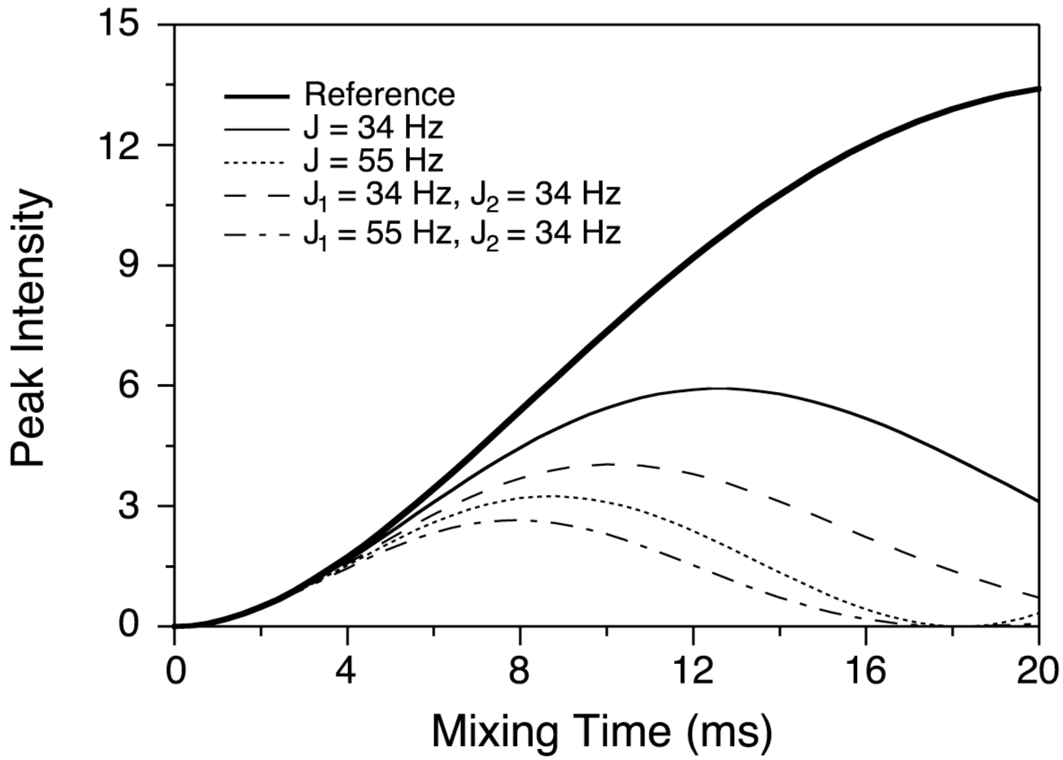

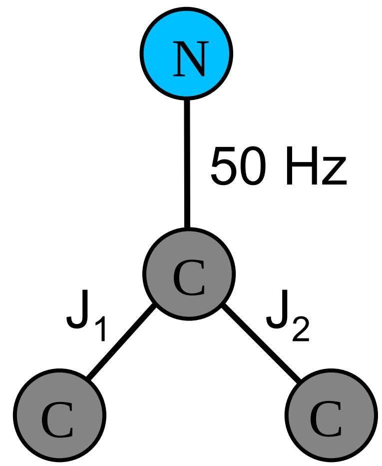

- ^{13}C-^{15}N cross-peak intensities reduced 2- to 5-fold

^{13}C Band-Selective 3D TEDOR Scheme

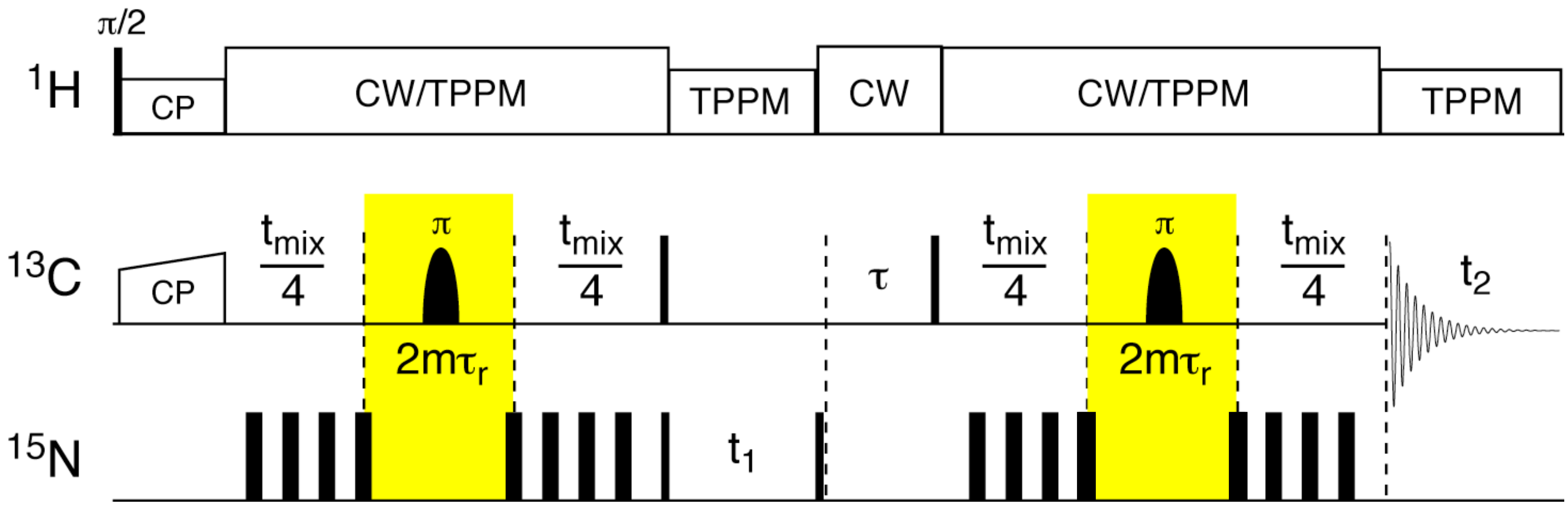

- ^{13}C-^{13}C J-couplings refocused using band-selective ^{13}C pulses (no z-filters required)
- Most useful for strongly J-coupled sites (e.g., C') but requires resolution in ^{13}C dimension

ZF-TEDOR vs. BASE-TEDOR

Gly $^{13}C\alpha$-^{15}N

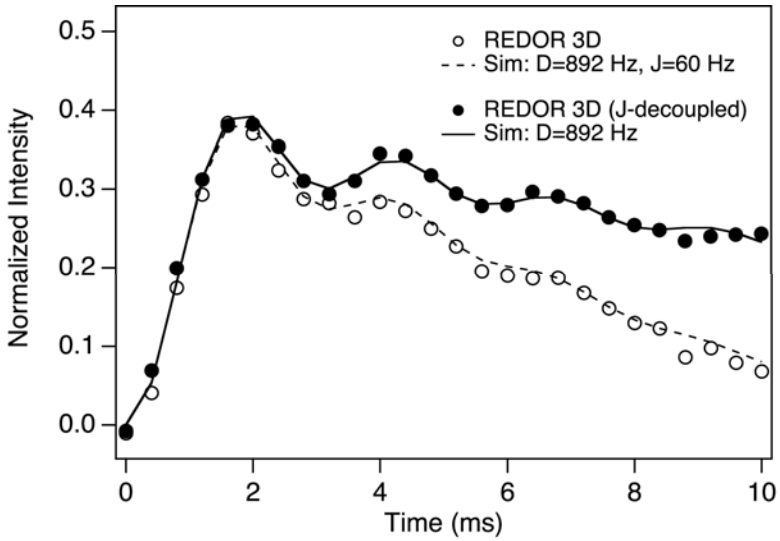

Gly $^{13}C'$-^{15}N

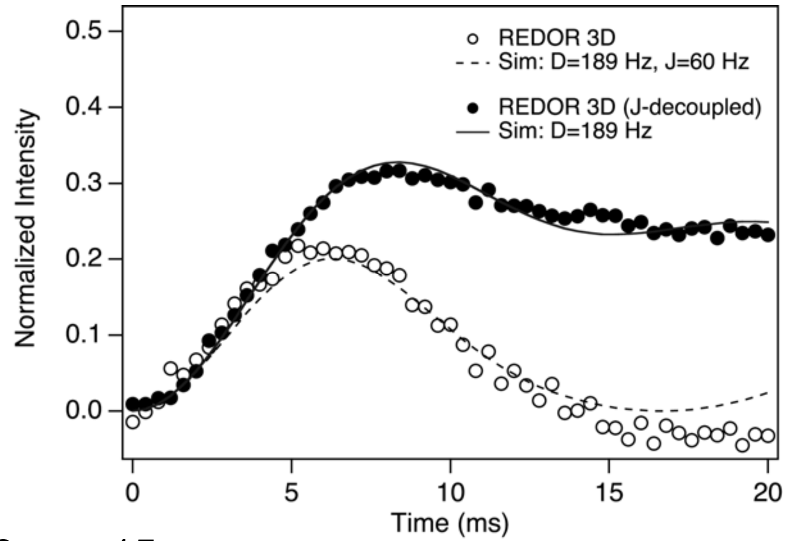

Thr $^{13}C\gamma$-^{15}N

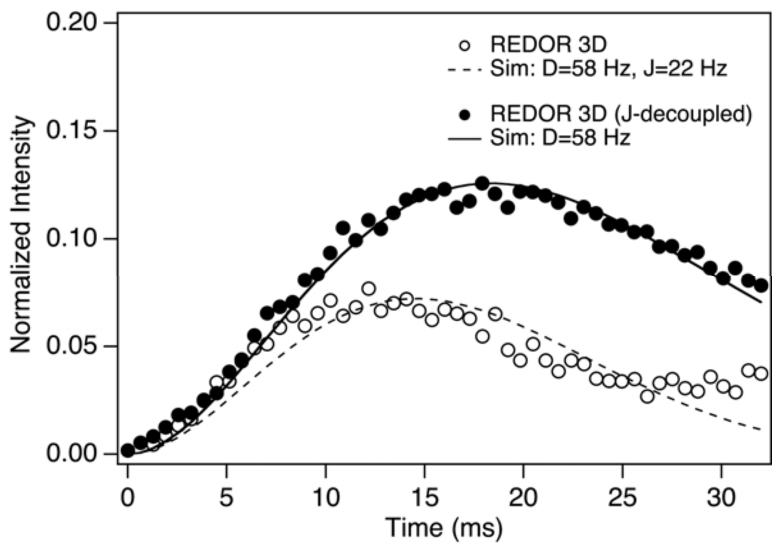

Cross-Peak Trajectories in TEDOR Expts.

3D ZF TEDOR

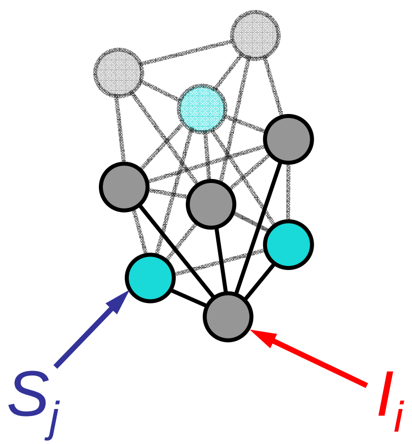

$$V_{ij} = V_i(0)\prod_{l\neq i}^{m_i}\cos^2\left(\pi J_{il}\tau\right)\times \left\langle \sin^2\left(\omega_{ij}\tau\right)\prod_{k\neq j}^{N_i}\cos^2\left(\omega_{ik}\tau\right)\right\rangle$$

3D BASE TEDOR

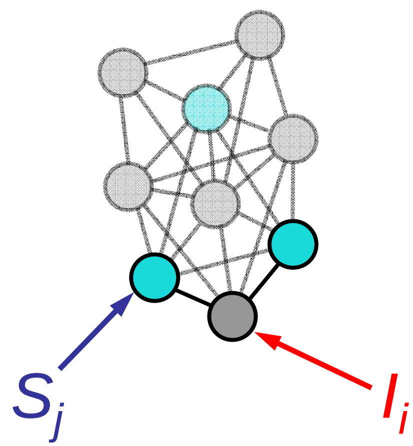

$$V_{ij} = V_i(0)\left\langle \sin^2\left(\omega_{ij}\tau\right)\prod_{k\neq j}^{N_i}\cos^2\left(\omega_{ik}\tau\right)\right\rangle$$

- Intensities depend on all spin-spin couplings to particular ^{13}C
- Use approximate models based on Bessel expansions of REDOR signals to describe cross-peak trajectories (**Mueller, *JMR* 1995**)

3D ZF-TEDOR: N-ac-VL

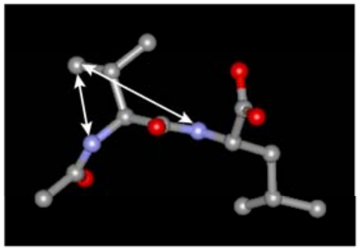

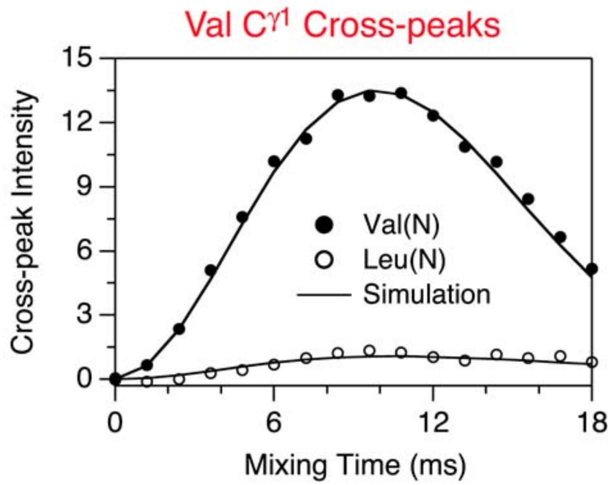

X-ray: 2.95 Å
NMR: 3.1 Å

Val(N)

X-ray: 4.69 Å
NMR: 4.7 Å

Leu(N)

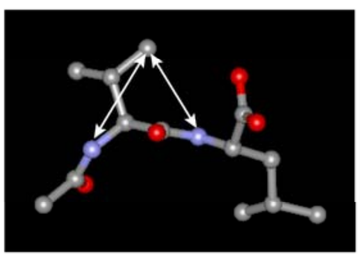

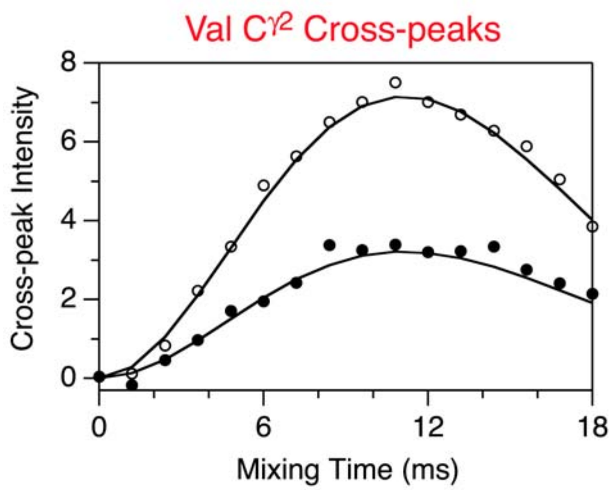

X-ray: 3.81 Å
NMR: 4.0 Å

Val(N)

X-ray: 3.38 Å
NMR: 3.5 Å

Leu(N)

3D BASE TEDOR: N-ac-VL

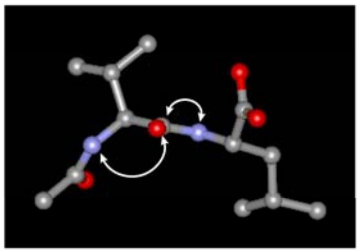

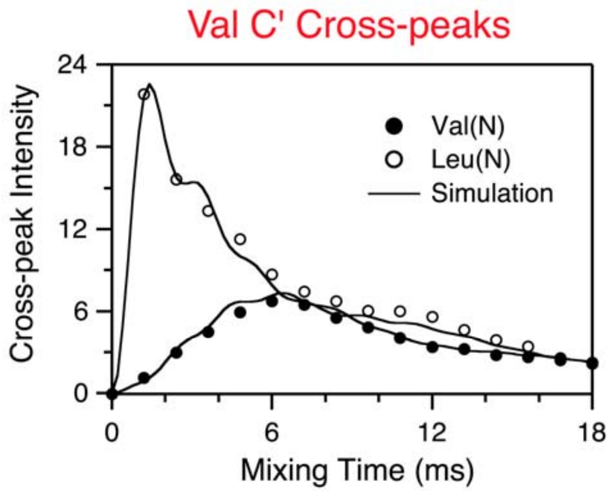

X-ray: 2.39 Å
NMR: 2.4 Å

Val(N)

X-ray: 1.33 Å
NMR: 1.3 Å

Leu(N)

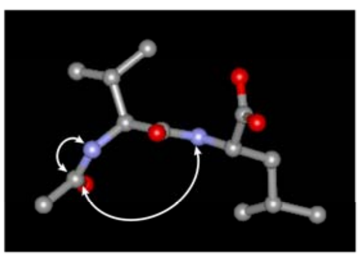

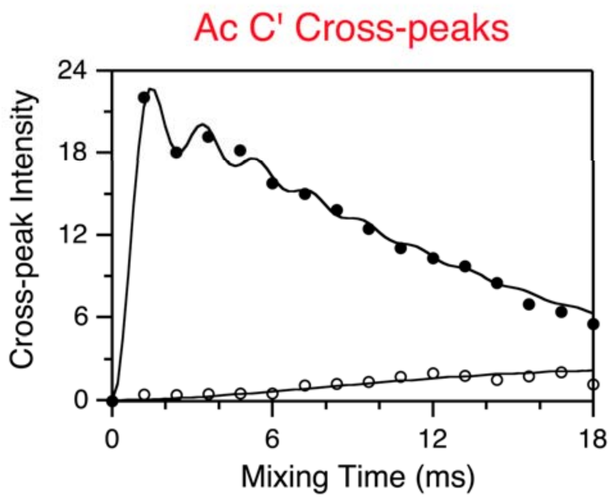

X-ray: 1.33 Å
NMR: 1.4 Å

Val(N)

X-ray: 4.28 Å
NMR: 4.1 Å

Leu(N)

Summary of Distance Measurements in N-ac-VL

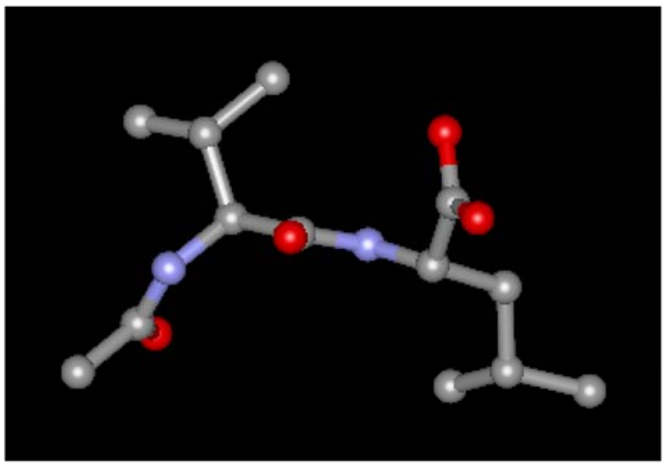

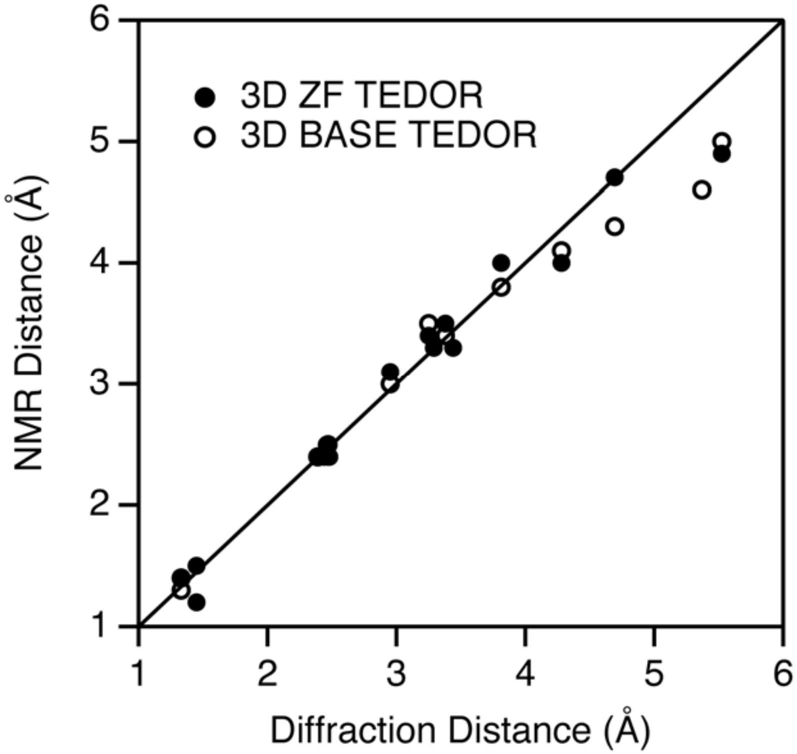

Application to TTR(105-115) Amyloid Fibrils

Slice from 3D ZF TEDOR Expt.

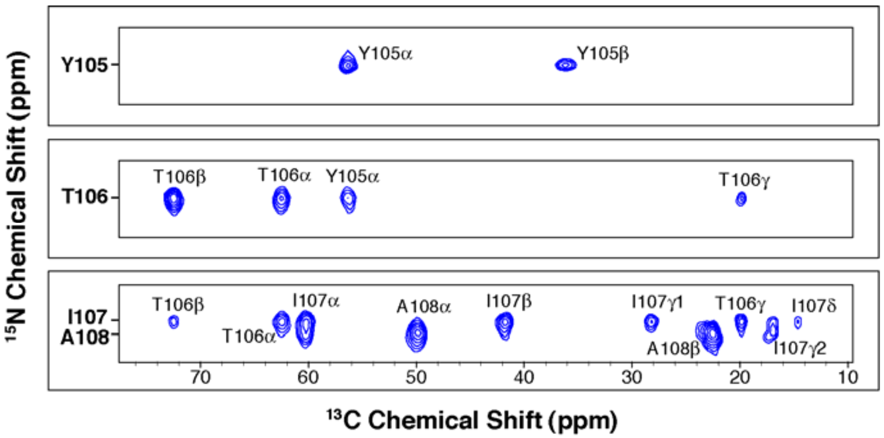

Cross-Peak Trajectories (T106)

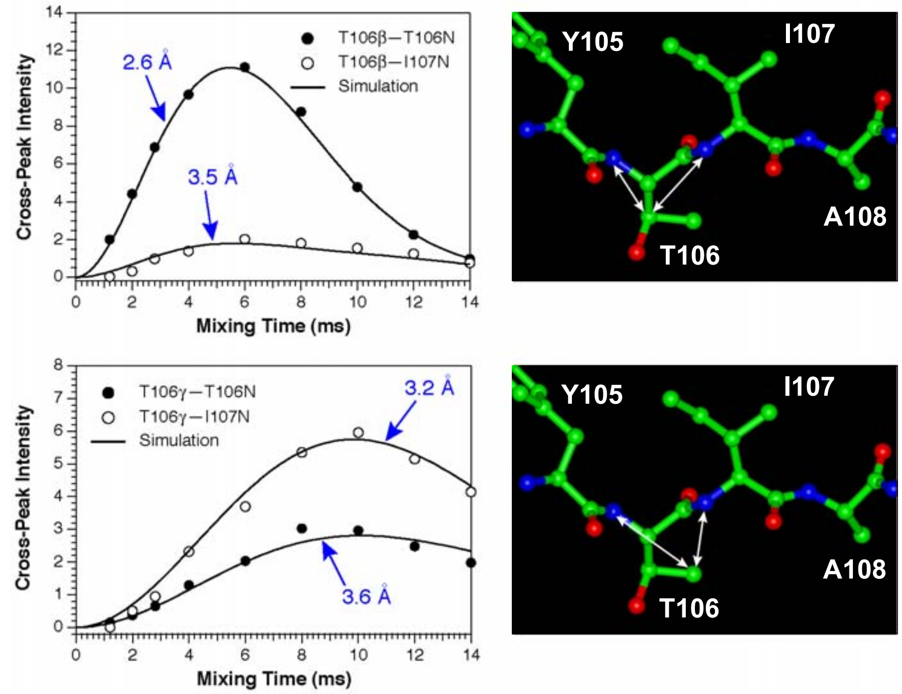

- ~70 ^{13}C-^{15}N distances measured by 3D ZF TEDOR in several U-^{13}C,^{15}N labeled fibril samples (30+ between 3-6 Å)

REDOR in Multispin Systems

$$\bar{H}_{IS} = \omega_1 2I_z S_{1z} + \omega_2 2I_z S_{2z}$$

$$I_x(t) = \left\langle \cos\left(\omega_1 t\right) \cos\left(\omega_2 t\right) \right\rangle$$

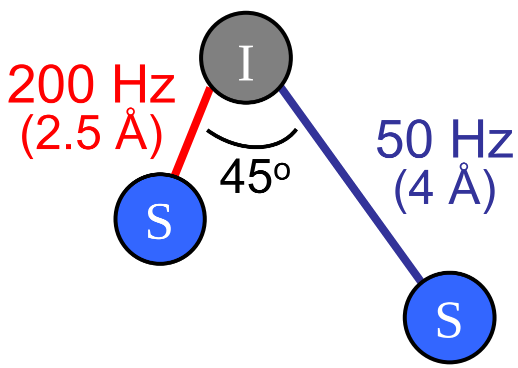

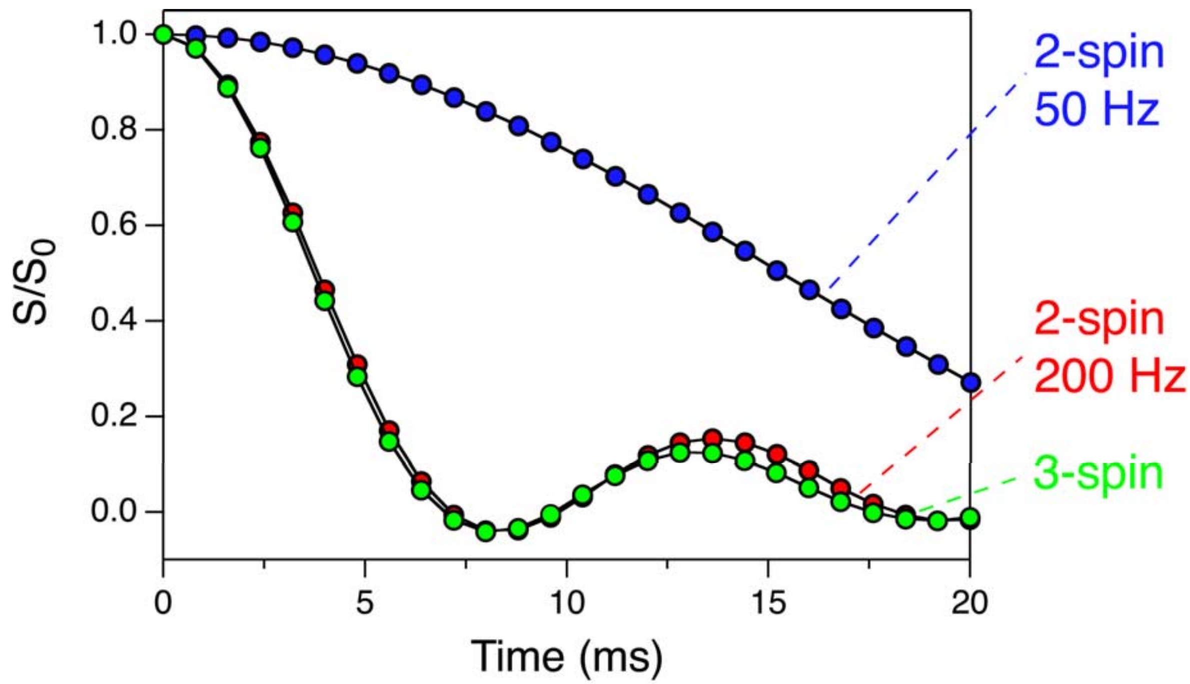

- Strong ^{13}C-^{15}N couplings dominate REDOR dipolar dephasing; weak couplings become effectively ‘invisible’

Dipole Tensor Correlation Experiments: Torsion Angles

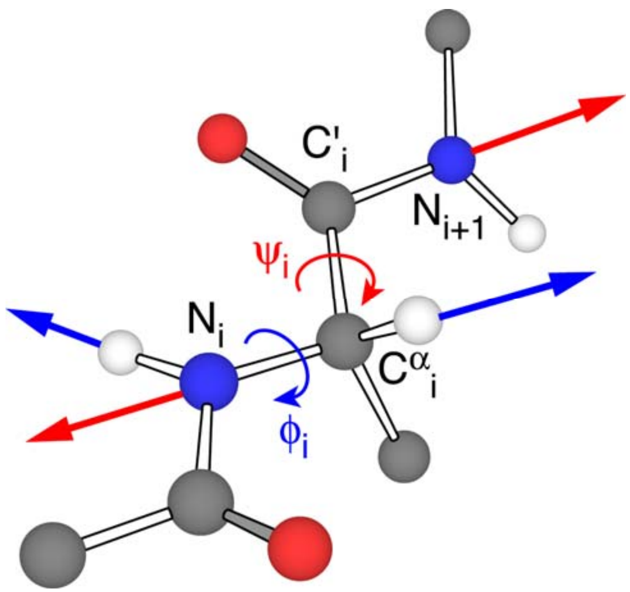

Observable signal

$$S(t) = \left\langle f_{mix} \cos(\Phi_1) \cos(\Phi_2) \right\rangle$$

$$\Phi_\lambda \equiv \Phi_\lambda(D_\lambda, \Omega_\lambda, t)$$

1. Torsion angle methods:
- Evolve a correlated spin state between two nuclei under their local dipolar fields
- Evolution highly sensitive to deviations from parallel arrangement of dipole vectors

2. Typical experiments:
- ^{1}H-^{15}N-$^{13}C^{\alpha}$-$^{1}H \Rightarrow \phi$
- ^{15}N-$^{13}C^{\alpha}$-$^{13}C'$-$^{15}N \Rightarrow \psi$
- ^{1}H-^{13}C-^{13}C-$^{1}H \Rightarrow \chi$

Measurement of ψ in Peptides

DQ-NCCN Pulse Sequence

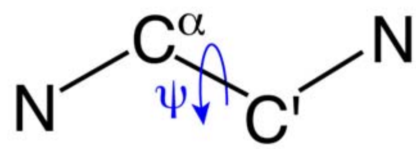

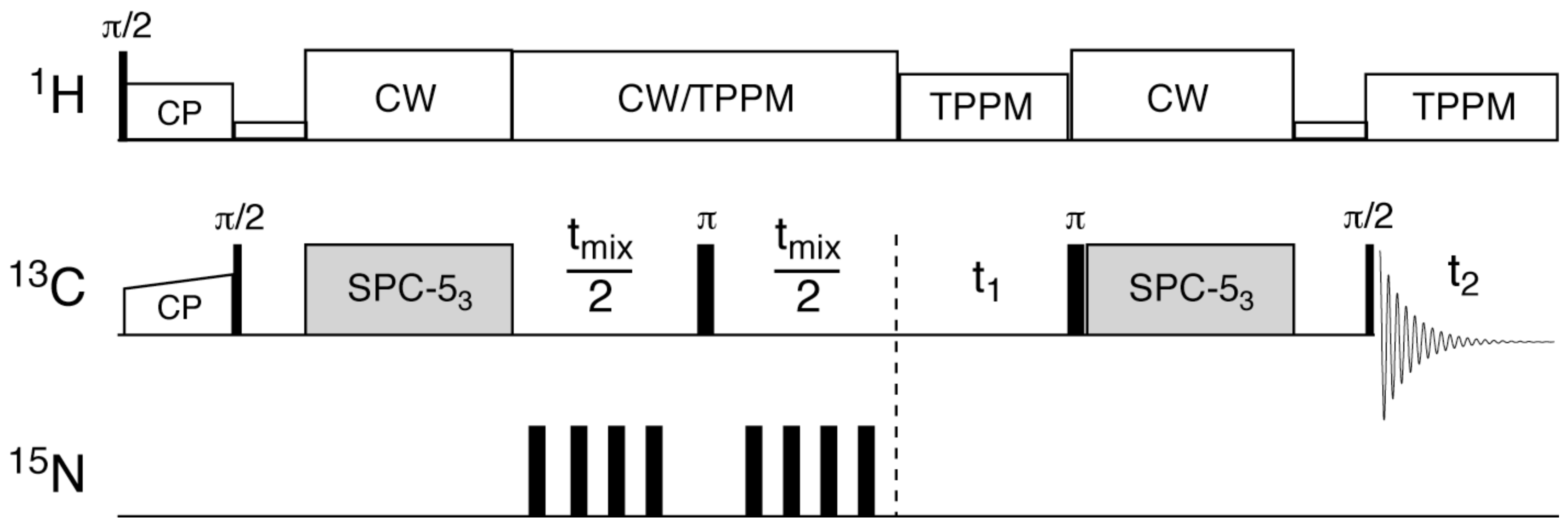

- ^{13}C-^{13}C DQC generated using SPC-5 (Hohwy *et al*. *JCP* 1999)
- ^{13}C-^{15}N dipolar interactions recoupled using REDOR

Costa, Gross, Hong & Griffin, *CPL* 1997
Levitt *et al*., *JACS* 1997

Dephasing Trajectories vs. ψ

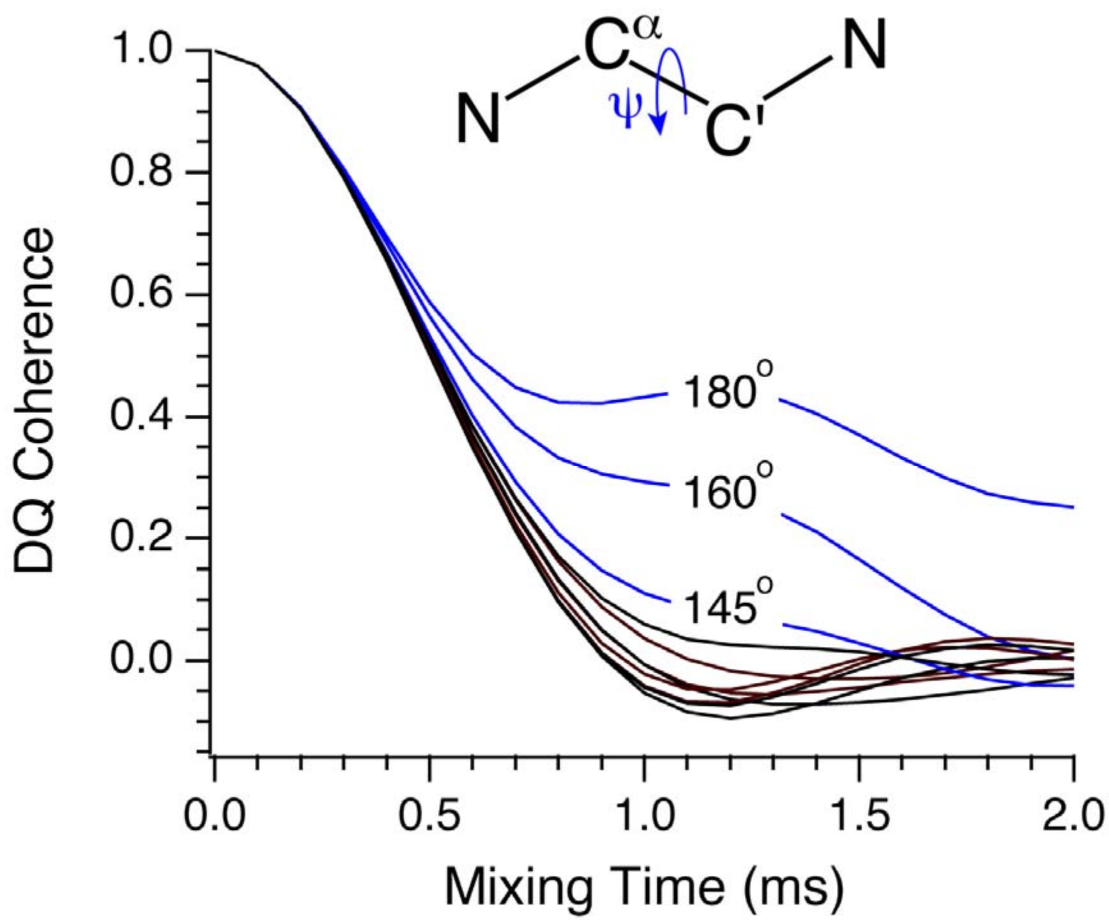

• Dephasing of ^{13}C-^{13}C DQ coherence is very sensitive to the relative orientation of ^{13}C-^{15}N dipolar tensors for $|\psi| \approx 150\text{-}180^o$

Application to TTR(105-115) Fibrils

Reference DQ-SQ correlation spectrum for U-^{13}C,^{15}N YTIA labeled sample

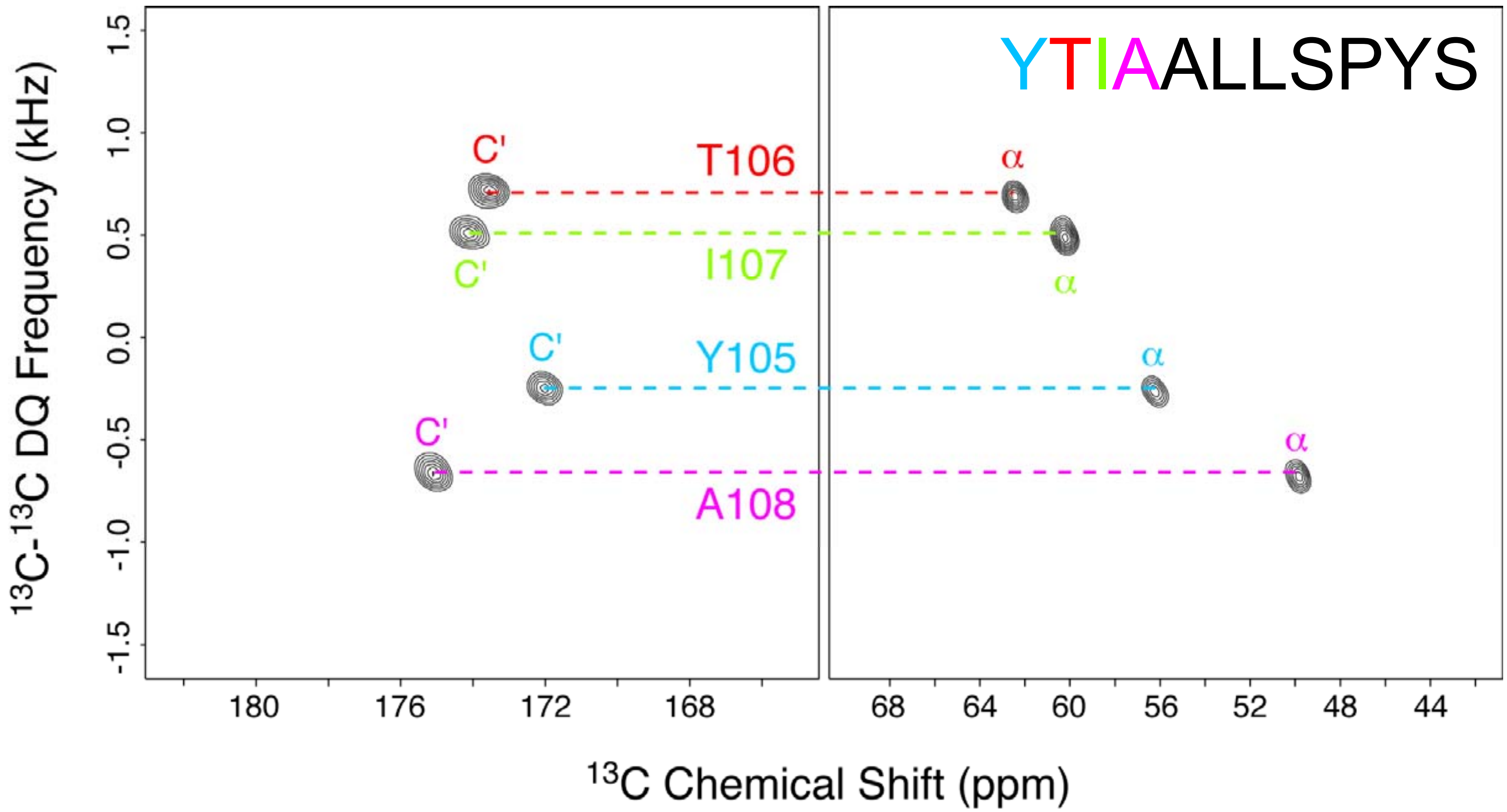

- ^{13}C-^{13}C DQ coherences evolve under the sum of CO and C$^{\alpha}$ resonance offsets during t_1

TTR(105-115): Dephasing Trajectories